Fermilab Library
0 1160 0049757 2

UCT-TP 226/95

Nucleon observables and loop diagrams in cavity QCD

FERMILAB
DEC 1995
LIBRARY

M. S. O'Connor
and
R. D. Viollier

Institute of Theoretical Physics and Astrophysics
University of Cape Town, Rondebosch 7700, South Africa

Abstract

Using a technique which is based on dimensional regularization, loop corrections to vertex diagrams of a massless quark moving in a spherical cavity are calculated in an arbitrary covariant gauge. Including the finite one-gluon-exchange diagrams, the corrections to the magnetic moments, vector and axial vector coupling constants, and the various r.m.s. radii of the nucleon are evaluated to order α_S. The results are compared with experimental data and previous calculations.

November 1995, to appear in *Annals of Physics (N.Y.)*

UCT-TP 226/95

1 Introduction

Over the past two decades, cavity QCD [1, 2] has been much used to gain a quantitative understanding of the properties of the hadrons. Similar to cavity QED which is the Abelian counterpart of cavity QCD, the boundary conditions that the fields must obey on a static sphere are consistent with the gauge symmetry and the field equations. Cavity QCD, as much as cavity QED, is therefore presumably a well-defined and renormalizable relativistic quantum field theory on its own, which could in principle be calculated perturbatively to arbitrary order. Apart from its non-Abelian character, the main feature that distinguishes cavity QCD from cavity QED is that the latter can be realized and observed in nature while it is still not clear whether perturbative cavity QCD provides a consistent framework for the description of the hadronic world.

One of the reasons for this deficiency is that the boundary conditions on the fields of the colour carrying particles are imposed in a somewhat arbitrary and *ad hoc* fashion, in order to mimic confinement, while confinement is generally believed to be a consequence of the dynamics of the non-Abelian gauge theory. Secondly, by confining particles to a static sphere, one breaks both, translational and Lorentz invariance of the underlying gauge theory, and it is difficult to restore these symmetries consistently without explicitly introducing the dynamics of the boundary, which necessarily amounts to solving the centre-of-mass problem exactly. Chiral symmetry is also broken, and this may be restored by introducing the coupling to an elementary pion field, as is done for instance in the chiral and cloudy bag models [3]. The price one has to pay for this remedy though, is that these chiral field theories are in general not renormalizable, which makes perturbative calculations dependent on a large number of renormalization parameters, with substantial loss of predictive power. Moreover, there remains the problem of double counting, as the pion can be treated both, as elementary and quark-antiquark degree of freedom. Thirdly, in the framework of cavity field theory, it is technically rather difficult to calculate higher-order Feynman diagrams [4], especially the diverging ones [5, 6, 7, 8, 9, 10], as the singularities have to be extracted numerically. While these higher-order corrections may be important,

they have been largely ignored in the past, with a few exceptions [5, 6, 7, 8, 9, 10]. Fourthly, it is by no means clear that perturbative cavity QCD will converge any better than ordinary free-space QCD. However, the fact that the field operators are expanded in cavity modes instead of plane waves helps at least to get rid of the infrared divergences plaguing free-space QCD. Indeed, a confined quark cannot radiate off a gluon as easily as a free quark, as the emitted gluon has a non-zero minimum mode energy.

Despite all of these shortcomings, it is important to investigate the higher-order predictions of cavity QCD in more detail, in order to establish whether perturbative cavity QCD makes sense as a possible description of the hadronic world. Thus, the purpose of this paper is to calculate all the $O(\alpha_S)$ diagrams, including loop diagrams, which contribute to the magnetic moments μ_p and μ_n, the vector and axial coupling constants g_V and g_A, and the root-mean-square radii $\langle r^2\rangle_p^{\frac{1}{2}}$, $\langle r^2\rangle_n^{\frac{1}{2}}$ and $\langle r^2\rangle_A^{\frac{1}{2}}$. Assuming that the nucleon contains only up and down quarks, we restrict our attention to massless quarks. We do not attempt to restore chiral symmetry, translational and Lorentz invariance, as this cannot be done in a model-independent way.

Recently, a reliable method for regularizing cavity loop-diagrams has been developed and applied to the self-energies of confined quarks [8, 11] and gluons [12], and the axial and vector coupling constant of the nucleon [9]. In this method, divergences due to the unreflected part of the propagators are extracted from loop integrals by using techniques similar to those of dimensional regularization in free space. In the case of the quark self-energy, Hansson and Jaffe [13, 14] have shown that the singular part of the loop integral is contained entirely in this free or un-reflected part of the quark propagator. Due to the Ward-Takahashi identities, this is also true for the vertex correction diagram which means that we can use the technique described in [8, 12] to calculate the $O(\alpha_S)$ vertex correction diagram in an arbitrary covariant gauge.

The paper is organized as follows: In the next chapter, we briefly review the calculation of the loop-corrections to the vertex diagram in free-space field theory, emphasizing those details which will be repeated in the analogous cavity calculation. In chapter 3, we use the Gell-Mann and Low theorem to obtain an expression for the

first-order corrections to the observables in question. Subsequently, we show in detail how to obtain the corrections to the magnetic moments. The results are discussed in chapter 4, while the calculational details are contained in the various appendices.

2 Vertex diagrams in free-space field theory

The three loop-diagrams that appear in a calculation of nucleon observables to order α_S (fig. 1) contain ultraviolet divergences which must be regularized before physically meaningful quantities can be extracted. After regularizing these diagrams, the sum is found to be gauge-independent in free-space field theory. For massless quarks, the singularities of the self-energy diagrams (fig. 1(b)–(c)) and the vertex diagrams (fig. 1(a)) cancel exactly. In the case of massive quarks, the self-energy diagrams develop an additional divergence which can be absorbed in a mass counter-term. For simplicity, we shall restrict ourselves here to massless up and down quarks.

Before attempting the regularization of these diagrams in cavity field theory, we note that the ultraviolet singularities are a high-momentum or short-distance phenomenon, and thus should have exactly the same structure for both confined and free particles. Additional divergences may arise in the cavity version due to the boundary conditions that are imposed at the surface of the cavity, although in the case of the quark self-energy, Hansson and Jaffe [13, 14] have shown that the M.I.T. boundary conditions do not introduce any new singularity. As the vertex correction and self-energy diagrams are intimately related through the Ward-Takahashi identities, the former is also free from boundary-induced divergences. This leads us to expect that the singularities of the cavity loop-diagrams will cancel, as well, and that the sum will be gauge-independent.

Let us begin with a brief review of the calculation of the one-loop correction to the vertex diagram in free-space field theory. In D dimensions, the vertex function $\Lambda^\mu(p',p,q)$ is given by

$$-i\Lambda^\mu(p',p,q) = g^2 \int \frac{d^Dk}{(2\pi)^D}(i\gamma_\alpha)\, iS(p'-k)(i\gamma^\mu)\, iS(p-k)(i\gamma_\beta)\, iD^{\alpha\beta}(k), \quad (1)$$

where we have omitted the arbitrary mass parameter, μ^{4-D}, which keeps the coupling constant g dimensionless. As the divergent part of $\Lambda^\mu(p',p,q)$ is independent of both the quark mass m and the momentum transfer q, m and q will be set to zero at the outset, for simplicity. Substituting the quark propagator and the gauge-independent part of the gluon propagator (i.e. the k^{-2} term) into eq. (1), one has

$$-i\Lambda^\mu(p,p) = \int \frac{d^Dk}{(2\pi)^D}\gamma_\alpha \frac{1}{\not p-\not k}\gamma^\mu \frac{1}{\not p-\not k}\gamma_\beta \frac{g^{\alpha\beta}}{k^2} = \int \frac{d^Dk}{(2\pi)^D}\frac{\gamma_\nu(\not p-\not k)\gamma^\mu(\not p-\not k)\gamma^\nu}{(p-k)^2(p-k)^2k^2}. \quad (2)$$

As we wish to carry over the method of evaluating this integral from free space to cavity field theory, it is convenient to review the details already here. After some Dirac algebra, one can rotate k and p to Euclidean space, i.e. $k^0 \to ik^0$ and $p^0 \to ip^0$, and elevate the denominators into the exponential using

$$\frac{1}{(p-k)^2} = \int_0^\infty dz\, e^{-z(p-k)^2} \quad (3)$$

for each factor in the denominator. Λ^μ may then be written as

$$-i\Lambda^\mu(p,p) = -i(2-D)\int \frac{d^Dk}{(2\pi)^D}\int_0^\infty dr \int_0^\infty ds \int_0^\infty dt \quad (4)$$
$$\times \left[2(\not p-\not k)(p-k)^\mu + \gamma^\mu(\not p-\not k)^2\right] e^{-rk^2-(s+t)(k-p)^2}.$$

Two successive shifts of variables can now be made

$$k \to k' + \frac{p(s+t)}{r+s+t} = k' + p - \frac{pr}{r+s+t} \quad (5)$$

$$r \to z(1-x-y) \quad , \quad s \to zx \quad , \quad t \to zy, \quad (6)$$

after which the exponent of eq. (4) becomes $zk'^2 + p^2z(x+y)(1-x-y)$. The integral over k' is now a standard Gaussian and may be evaluated immediately to yield

$$-i\Lambda^\mu(p,p) = -i(2-D)\int_0^1 dx \int_0^{1-x} dy \int_0^\infty dz\, z^2 \left(\frac{1}{4\pi z}\right)^{D/2} \quad (7)$$
$$\times \left[\frac{\gamma^\mu}{z}\left(1-\frac{D}{2}\right) + (1-x-y)^2(2\not p p^\mu - \gamma^\mu p^2)\right] e^{-zp^2(x+y)(x+y-1)},$$

where the result has been rotated back into Minkowski space. Setting $D = 4-2\epsilon$, where ϵ is small, and evaluating the remaining integrals, one arrives at

$$-i\Lambda^\mu(p,p) = -\frac{i}{16\pi^2}\left[\gamma^\mu\left(\frac{1}{\epsilon} - \gamma + 1 - \ln(-p^2/4\pi)\right) - \frac{2\not p p^\mu}{p^2}\right], \quad (8)$$

where γ is Euler's constant. Using the integral representation of the gamma function, the singular part of Λ^μ in 4-dimensional space may be parametrized as

$$-i\Lambda^\mu_S = -\frac{i\gamma^\mu}{16\pi^2}\int_0^\infty dz\, \frac{e^{-z}}{z}. \quad (9)$$

The self-energy of the quark, $\Sigma(p)$, which is related to the vertex function through the Ward identity, $\Lambda^\mu(p,p) = \partial\Sigma(p)/\partial p_\mu$, can be calculated in exactly the same manner, yielding

$$i\Sigma(p) = -\frac{i\not{p}}{16\pi^2}\left[\frac{1}{\epsilon} - \gamma + 1 - \ln(-p^2/4\pi)\right] \tag{10}$$

for massless quarks. The singular part of the self-energy is

$$i\Sigma_S(p) = -\frac{i\not{p}}{16\pi^2}\int_0^\infty dz\,\frac{e^{-z}}{z} = B\not{p}, \tag{11}$$

where B denotes the divergent constant $-i\Gamma(\epsilon)/16\pi^2$. Calculating the amplitude of the self-energy inserts, we encounter a difficulty which will also occur in cavity field theory. As the method of resolving this problem is the same in both, free-space and cavity field theory, it is convenient to discuss it already here. The Feynman amplitude $\mathcal{M}^b$ for the self-energy diagram (fig. 1(b)) is given by

$$\mathcal{M}^b = g^2 C\,\bar{u}(p')\,i\gamma_\mu\,iS(p)i\Sigma(p)\,u(p)A^\mu_{\rm ext}(q), \tag{12}$$

where $C = 4/3$ is a colour factor and $A^\mu_{\rm ext}(q)$ is some external potential. Inserting the quark propagator and the singular part of $\Sigma(p)$ into eq.(12), we arrive at

$$\mathcal{M}^b_S = ig^2 C\,\bar{u}(p')\,\gamma_\mu\frac{1}{\not{p}}B\not{p}u(p)A^\mu_{\rm ext}(q) \tag{13}$$

which is ill-defined, as evident from the fact that the on-shell value of $\not{p}/\not{p}$ is of the form 0/0. Alternatively, the result of $\not{p}$ acting on a free-particle spinor $u(p)$ is zero, while if the $\not{p}$'s in the numerator and denominator are allowed to cancel before acting on the spinor, the result is proportional to $u(p)$. This difficulty can be resolved by adiabatically 'switching-on' the interaction, introducing a function $g(t)$, which tends to zero as $t \to \pm\infty$, and is of unit value for $t = 0$. Fourier transforming $g(t)$ into energy space,

$$g(t) = \int_{-\infty}^{\infty} dE\,G(E)e^{iEt}, \tag{14}$$

$G(E)$ turns out to be almost a δ-function, with the normalization $g(0) = \int dE\,G(E) = 1$. Including the Fourier-transformed damping factor in the interaction Hamiltonian, the self-energy and quark propagator are replaced by

$$\Sigma(p) \to \Sigma(p-s) \quad , \quad \frac{1}{\not{p}} \to \frac{1}{\not{p}-\not{s}-\not{s}'}$$

and the Feynman amplitude (13) becomes

$$\mathcal{M}^b_S = ieg^2 C\bar{u}(p')\int dE\,dE'\,G(E)G(E')\,\gamma_\mu\frac{1}{\not{p}-\not{s}-\not{s}'}B(\not{p}-\not{s})\,u(p)A^\mu_{\rm ext}(q). \tag{15}$$

One way of evaluating the integral is to subtract a factor of $\frac{1}{2}\not{p}u(p)$ from the numerator, which may be done since $\not{p}u(p) = 0$. This allows us to make the substitution

$$(\not{p}-\not{s}) \to (\not{p}-\not{s}) - \tfrac{1}{2}\not{p} = \tfrac{1}{2}(\not{p} - 2\not{s}).$$

Furthermore, the factor of $2\not{s}$ may be symmetrized by making the replacement $2\not{s} \to \not{s}+\not{s}'$. The integral now straight-forwardly yields

$$\mathcal{M}^b_S = ig^2 C\,\bar{u}(p')\,\frac{\gamma_\mu B}{2}\,u(p)A^\mu_{\rm ext}(q). \tag{16}$$

The factor of $\frac{1}{2}B$ is particularly important since the same result holds for the diagram shown in fig. 1(c), hence the sum of these two terms contains a factor of exactly B.

The Feynman amplitude $\mathcal{M}^a_S$ for the singular part of the vertex correction can be found immediately from eq. (9), yielding

$$\mathcal{M}^a_S = -ig^2 C\,\bar{u}(p')\,\gamma_\mu B\,u(p)A^\mu_{\rm ext}(q). \tag{17}$$

This cancels exactly the singularities arising from the self-energy inserts.

So far, we have discussed the term proportional to k^{-2} rather than the full gluon-propagator. If the remaining term in the propagator, which depends on gauge parameter, is now inserted into the Feynman amplitudes for these diagrams, one finds that the sum of the three amplitudes vanishes identically, i.e. the sum of these diagrams is gauge-independent.

3 Vertex diagrams in cavity field theory

3.1 Perturbation expansion

Assuming that perturbation theory is valid, cavity QCD can, as its free-space counterpart, be expanded as a perturbation series in the strong coupling constant g. Using the Gell-Mann and Low theorem, this approach leads to a perturbative expansion of the energy shift due to the interaction [15, 23]

$$\Delta E_k = \lim_{\epsilon\to 0} \frac{\left\langle \hat{\phi}_k \middle| \hat{H}^{\epsilon}_{int}(0)\hat{U}^{\epsilon}(-\infty,0) \middle| \hat{\phi}_k \right\rangle_c}{\left\langle \hat{\phi}_k \middle| \hat{U}^{\epsilon}(-\infty,0) \middle| \hat{\phi}_k \right\rangle_c}. \tag{18}$$

The subscript c indicates that only connected diagrams are included, and $|\hat{\phi}_k>$ is an eigenvector of the non-interacting Hamilton operator. The time-evolution operator $\hat{U}(t,t_0)$ is defined in terms of the interaction Hamiltonian $\hat{H}_{int}(t)$ and Wick's time-ordered product T by

$$\hat{U}^{\epsilon}(-\infty,0) = \sum_{n=0}^{\infty} \frac{(-i)^n}{n!} \int_{-\infty}^{0} dt_1 \cdots \int_{-\infty}^{0} dt_n\, T\left[\hat{H}^{\epsilon}_{int}(t_1)\cdots \hat{H}^{\epsilon}_{int}(t_n)\right]. \tag{19}$$

Since, to order g^2, the three-gluon, four-gluon and ghost-gluon vertices do not contribute to the nucleon, the interaction Hamiltonian is simply given by the term describing the quark-gluon vertex, i.e.

$$\hat{H}^{\epsilon}_{int}(t) \;=\; -ge^{-\epsilon|t|}\int d^3x\, \hat{\mathcal{H}}(x) \;=\; -ge^{-\epsilon|t|}\int d^3x\, \hat{\bar{\psi}}(x)\frac{\lambda_a}{2}\hat{\not{A}}_a(x)\hat{\psi}(x), \tag{20}$$

where $e^{-\epsilon|t|}$ is the adiabatic damping factor, $\hat{\psi}(x)$ the quark field operator, $\hat{A}^{\mu}_a(x)$ the vector field operator describing the gluons, and the λ_a's are the Gell-Mann matrices.

Writing the Gell-Mann and Low theorem in this form, Feynman diagrams may be decomposed into time-ordered diagrams, each of which needs to be evaluated separately. This undesirable feature can be avoided using a more symmetric form of the Gell-Mann and Low theorem [16], where the energy shifts are given in terms of the dummy variable ξ by

$$\Delta E_k = \lim_{\substack{\xi\to 1\\ \epsilon\to 0}} \frac{i\epsilon}{2}\, \frac{\partial\left\langle \hat{\phi}_k \middle| S_{\epsilon,\xi} \middle| \hat{\phi}_k \right\rangle_c \Big/ \partial\xi}{\left\langle \hat{\phi}_k \middle| S_{\epsilon,\xi} \middle| \hat{\phi}_k \right\rangle_c}. \tag{21}$$

The adiabatic S-matrix $S_{\epsilon,\xi}$ can be expanded as $S_{\epsilon,\xi} \equiv 1 + \sum_{n=1}^{\infty} S^{(n)}_{\epsilon,\xi}$,

$$S^{(n)}_{\epsilon,\xi} = \frac{(-i\xi)^n}{n!}\int_{-\infty}^{\infty} dt_1 \cdots \int_{-\infty}^{\infty} dt_n\, e^{-\epsilon|t_1|}\cdots e^{-\epsilon|t_n|}\, T\left[\hat{H}_{int}(t_1)\cdots \hat{H}_{int}(t_n)\right]. \tag{22}$$

Since the limits in the time integrations appearing in the S-matrix are symmetric, all the time-ordered diagrams of a given Feynman diagram are equivalent, and there is no need to decompose a Feynman diagram into its constituent time-ordered graphs. However, the price one pays for this convenience is that the time integrations are more difficult to perform.

The nucleon observables which will be calculated in this work are all given by the expectation values of one-body operators. The five operators $\mathcal{O}$ which we shall discuss here are

$r^2\gamma_0 Q$	charge radius squared	
$\frac{1}{2}(\vec{r}\times\vec{\gamma})_3 Q$	magnetic moment	
$\gamma_0 Q$	vector coupling constant	(23)
$\gamma_3\gamma_5\tau_3$	axial vector coupling constant	
$r^2\gamma_3\gamma_5\tau_3$	axial vector radius squared,	

where Q is the charge matrix of the flavoured quarks. To $O(g^2)$, the value of the observable $\mathcal{O}$ is given by $\mathcal{O} = \mathcal{O}^{(0)} + \mathcal{O}^{(2)}$, where

$$\mathcal{O}^{(0)} = \int d^4x \left\langle \hat{N} \middle| \hat{\bar{\psi}}(x)\hat{\mathcal{O}}(x)\hat{\psi}(x) \middle| \hat{N} \right\rangle \tag{24}$$

is the zero'th order term. Starting with the symmetric form of the Gell-Mann and Low theorem, the second order term $\mathcal{O}^{(2)}$ is found to be

$$\mathcal{O}^{(2)} = \lim_{\epsilon\to 0} g^2 \frac{3i\epsilon}{2}\frac{(-i)^3}{3!}\int d^4x_1 \int d^4x_2 \int d^4x_3\, e^{-\epsilon(|t_1|+|t_2|+|t_3|)} \times \tag{25}$$

$$\left\langle \hat{N} \middle| T\left[\left(\hat{\bar{\psi}}(x_1)\frac{\lambda_a}{2}\hat{\not{A}}_a(x_1)\hat{\psi}(x_1)\right)\left(\hat{\bar{\psi}}(x_2)\hat{\mathcal{O}}(x_2)\hat{\psi}(x_2)\right)\left(\hat{\bar{\psi}}(x_3)\frac{\lambda_b}{2}\hat{\not{A}}_b(x_3)\hat{\psi}(x_3)\right)\right] \middle| \hat{N} \right\rangle_c,$$

where $|\hat{N}\rangle$is the appropriate nucleon wavefunction. Using Wick's theorem, the time-ordered product of the fields is contracted in all possible ways to yield the sum of normal-ordered products. Of these, some are not connected to $|\hat{N}\rangle$ and can thus be discarded. The remaining terms with the same spatial structure may then be collected in groups of 6, represented by the Feynman diagrams shown in fig. 2.

3.2 Vertex correction

Let us consider the contribution $\mu_{\mathbf{a}}^{(2)}$ of the vertex correction graph (fig. 2(a)) to the magnetic moment. From eq. (25), we have

$$\mu_{\mathbf{a}}^{(2)} = \lim_{\epsilon\to 0} g^2 \frac{3i\epsilon}{2}\frac{(-i)^3}{3!}\int d^4x_1 \int d^4x_2 \int d^4x_3\, e^{-\epsilon(|t_1|+|t_2|+|t_3|)} \tag{26}$$
$$\times\left\langle \hat{N}\left|\left(\bar{\psi}\frac{\lambda_a}{2}\not{A}_a\psi\right)_{x_1}\left(\bar{\psi}(\vec{x}_2\times\vec{\gamma})_3 Q\psi\right)_{x_2}\left(\bar{\psi}\frac{\lambda_b}{2}\not{A}_b\psi\right)_{x_3}\right|\hat{N}\right\rangle,$$

where one of the possible contractions has been indicated. Since the limits of the time integrals are symmetric, the 6 possible permutations of the space-time labels x_1, x_2 and x_3 are equivalent. We therefore may use the one contraction shown above and omit the factor of 1/3!, thus including all the permutations.

The gluon propagator can be divided into a part independent of the gauge parameter (equivalent to the Feynman-gauge propagator), and the remainder, which depends explicitly on the gauge parameter. This latter part will be used later to show that the result is gauge-independent. Substituting the former into eq. (26), and inserting the quark propagator (76) from appendix A, and the cavity mode expansion of the fields, the gauge-independent part of $\mu_{\mathbf{a}}^{(2)}$ becomes

$$\mu_{\mathbf{a}}^{(2)} = \lim_{\epsilon\to 0}\frac{3i\epsilon}{2} g^2 \sum_{\substack{pqm\Sigma\\ cc'ff'nn'}} \left\langle \hat{N}\left|\hat{a}^\dagger_{c'f'n'}\left(\frac{\lambda^a}{2}\right)_{c'd}\left(\frac{\lambda^a}{2}\right)_{dc} Q\,\hat{a}_{cfn}\right|\hat{N}\right\rangle \int d^3x_2\, \bar{u}_p(x_2)(\vec{x}_2\times\vec{\gamma})_3 u_q(x_2)$$
$$g^{\Sigma\Sigma}\int d^3x_1\, \bar{u}_{n'}(x_1)\gamma_\mu u_p(x_1) a^{\mu *}_{m\Sigma}(x_1)\int d^3x_3\, \bar{u}_q(x_3)\gamma_\nu u_n(x_3) a^\nu_{m\Sigma}(x_3)$$
$$\int dt_1\, dt_2\, dt_3 \int \frac{d\omega}{2\pi}\frac{d\omega'}{2\pi}\frac{d\omega''}{2\pi}\frac{e^{-\epsilon(|t_1|+|t_2|+|t_3|)}\, e^{it_1(\varepsilon_{n'}+\omega-\omega')}\, e^{it_2(\omega'-\omega'')}\, e^{it_3(\omega''-\omega-\varepsilon_n)}}{(\omega'-\varepsilon_p\pm i0)(\omega''-\varepsilon_q\pm i0)(\omega^2-\Omega^2+i0)}. \tag{27}$$

To reduce the proliferation of indices, the energy of the intermediate gluon has been written as Ω instead of Ω_m^Σ. The $\pm i0$ prescription will henceforth be assumed in the propagators, as will the summation over the labels $c'f'n'$ and cfn (i.e. colour, flavour and cavity modes). The expectation value of the colour, charge and creation/annihilation operators is given in appendix E, and will be discarded from the formulae until needed. Writing the vertex integrals over the space co-ordinates in the

short-hand form introduced in appendix B, eqs. (102) and (114), the vertex correction to the magnetic moment, eq. (27), can be expressed more compactly as

$$\mu_{\mathbf{a}}^{(2)} = \lim_{\epsilon\to 0}\frac{3i\epsilon}{2} g^2 \sum_{pqm\Sigma} g^{\Sigma\Sigma}\,\tilde{Q}^{m\Sigma}_{n'p}\, M_{pq}\, Q^{m\Sigma}_{qn} \tag{28}$$
$$\int_{-\infty}^{\infty} dt_1\, dt_2\, dt_3 \int_{-\infty}^{\infty}\frac{d\omega}{2\pi}\frac{d\omega'}{2\pi}\frac{d\omega''}{2\pi}\frac{e^{-\epsilon(|t_1|+|t_2|+|t_3|)}\, e^{it_1(\varepsilon_{n'}+\omega-\omega')}\, e^{it_2(\omega'-\omega'')}\, e^{it_3(\omega''-\omega-\varepsilon_n)}}{(\omega'-\varepsilon_p)(\omega''-\varepsilon_q)(\omega^2-\Omega^2)}.$$

The integrals $\int dt_1\, dt_2\, dt_3 \int d\omega'\, d\omega''$ can be evaluated immediately to give

$$\mu_{\mathbf{a}}^{(2)} = ig^2 \sum_{pqm\Sigma} g^{\Sigma\Sigma}\,\tilde{Q}^{m\Sigma}_{n'p}\, M_{pq}\, Q^{m\Sigma}_{qn}\int\frac{d\omega}{2\pi}\frac{\delta(\varepsilon_n,\varepsilon_{n'})}{(\varepsilon_{n'}+\omega-\varepsilon_p)(\varepsilon_n+\omega-\varepsilon_q)(\omega^2-\Omega^2)}, \tag{29}$$

where $\delta(\varepsilon_n,\varepsilon_{n'})$ is the Kronecker delta implying $n=n'$. The integral over ω is analogous to the free-particle integral over the gluon momentum k^0. It can be evaluated in two ways: either as a contour integral, producing an energy denominator, or with the dimensional regularization techniques used in free-space field theory. The latter method enables the cavity vertex correction to be regularized by parametrizing its divergence.

The integral in eq. (29) is easily evaluated by the first method, i.e. as a contour integral, yielding

$$I^{m\Sigma}_{pq} \equiv i\int\frac{d\omega}{2\pi}\frac{1}{(\varepsilon_n+\omega-\varepsilon_p)(\varepsilon_n+\omega-\varepsilon_q)(\omega^2-\Omega^2)} \tag{30}$$

$$= \begin{cases} \dfrac{1}{2\Omega(\varepsilon_n-\Omega\,\mathrm{sgn}\varepsilon_p-\varepsilon_p)(\varepsilon_n-\Omega\,\mathrm{sgn}\varepsilon_q-\varepsilon_q)} & \text{if } \mathrm{sgn}\varepsilon_p=\mathrm{sgn}\varepsilon_q \\[2ex] \dfrac{-(2\Omega+\varepsilon_p+\varepsilon_q)}{2\Omega(\varepsilon_n-\Omega\,\mathrm{sgn}\varepsilon_p-\varepsilon_p)(\varepsilon_n-\Omega\,\mathrm{sgn}\varepsilon_q-\varepsilon_q)(\varepsilon_p+\varepsilon_q)} & \text{if } \mathrm{sgn}\varepsilon_p\neq\mathrm{sgn}\varepsilon_q \end{cases}. \tag{31}$$

When this result is inserted into eq. (29), the vertex correction is expressed purely as a sum of vertex integrals, weighted by an energy denominator, and it diverges logarithmically. This is the form in which cavity diagrams are usually evaluated, since it arises naturally when the unsymmetric version of the Gell-Mann and Low theorem is used.

Let us now proceed to evaluate $I^{m\Sigma}_{pq}$ as it would be done in free-space field theory. Reducing the $\pm i0$ prescription to $+i0$ in the denominator by squaring the quark

propagator pieces, Wick-rotating to Euclidean space with the shifts $\omega \to i\omega$ and $\varepsilon_n \to i\varepsilon_n$, and elevating the denominators into the exponential, $I_{pq}^{m\Sigma}$ becomes

$$I_{pq}^{m\Sigma} = \int \frac{d\omega}{2\pi}\Big[\varepsilon_p + i(\omega+\varepsilon_n)\Big]\Big[\varepsilon_q + i(\omega+\varepsilon_n)\Big] \times \int_0^\infty dr \int_0^\infty ds \int_0^\infty dt\, e^{-r(\omega^2+\Omega^2)}\, e^{-s\left[(\varepsilon_n+\omega)^2+\varepsilon_p^2\right]}\, e^{-t\left[(\varepsilon_n+\omega)^2+\varepsilon_q^2\right]}. \tag{32}$$

Making shifts of variables comparable to those used in free-space field theory, eqs. (5) and (6), i.e.

$$r \to z(1-x-y) \quad , \quad s \to zx \quad , \quad t \to zy \quad , \quad \omega \to \omega - \varepsilon_n(x+y), \tag{33}$$

we arrive at

$$I_{pq}^{m\Sigma} = \int \frac{d\omega}{2\pi}\int_0^\infty dz\, z^2 \int_0^1 dx \int_0^{1-x} dy \Big[\varepsilon_p + i\varepsilon_n(1-x-y) + i\omega\Big] \times \Big[\varepsilon_q + i\varepsilon_n(1-x-y) + i\omega\Big]\, e^{-z\left[\omega^2+\Omega^2(1-x-y)+\varepsilon_n^2(x+y)(1-x-y)+x\varepsilon_p^2+y\varepsilon_q^2\right]}. \tag{34}$$

The ω integral is a standard Gaussian, yielding, after rotating back to Minkowski space,

$$I_{pq}^{m\Sigma} = \int_0^\infty dz \int_0^1 dx \int_0^{1-x} dy \left[\Big(\varepsilon_p + \varepsilon_n(1-x-y)\Big)\Big(\varepsilon_q + \varepsilon_n(1-x-y)\Big) z - \frac{1}{2}\right] \times \sqrt{\frac{z}{4\pi}}\, e^{-z\left[\Omega^2(1-x-y)-\varepsilon_n^2(x+y)(1-x-y)+x\varepsilon_p^2+y\varepsilon_q^2\right]}. \tag{35}$$

Finally, evaluating the integrals over the x- and y variables, and writing $I_{pq}^{m\Sigma} = \int_0^\infty dz\, I_{pq}^{m\Sigma}(z)$, we obtain

$$\begin{aligned} I_{pq}^{m\Sigma}(z) = {} & \frac{(\varepsilon_n+\varepsilon_q)^2 - \Omega^2 + 2\varepsilon_n\varepsilon_p}{8\varepsilon_n^2(\varepsilon_q^2-\varepsilon_p^2)\sqrt{\pi z}}\, e^{-z\varepsilon_q^2} - \frac{(\varepsilon_n+\varepsilon_p)^2 - \Omega^2 + 2\varepsilon_n\varepsilon_q}{8\varepsilon_n^2(\varepsilon_q^2-\varepsilon_p^2)\sqrt{\pi z}}\, e^{-z\varepsilon_p^2} - \frac{e^{-z\Omega^2}}{8\varepsilon_n^2\sqrt{\pi z}} \\ & + \frac{(\varepsilon_n^2+\varepsilon_q^2-\Omega^2+2\varepsilon_n\varepsilon_p)[(\varepsilon_n+\varepsilon_q)^2-\Omega^2]}{16\varepsilon_n^3(\varepsilon_q^2-\varepsilon_p^2)}\Big[e^{-z\Omega^2}\mathrm{nerf}\left(\sqrt{z}\,A_+\right) + e^{-z\varepsilon_q^2}\mathrm{nerf}\left(\sqrt{z}\,A_-\right)\Big] \\ & - \frac{(\varepsilon_n^2+\varepsilon_p^2-\Omega^2+2\varepsilon_n\varepsilon_q)[(\varepsilon_n+\varepsilon_p)^2-\Omega^2]}{16\varepsilon_n^3(\varepsilon_q^2-\varepsilon_p^2)}\Big[e^{-z\Omega^2}\mathrm{nerf}\left(\sqrt{z}\,B_+\right) + e^{-z\varepsilon_p^2}\mathrm{nerf}\left(\sqrt{z}\,B_-\right)\Big], \end{aligned} \tag{36}$$

where the normalized error function $\mathrm{nerf}(x)$ is defined by

$$\mathrm{nerf}(x) = \frac{2}{\sqrt{\pi}}\, e^{x^2}\int_0^x e^{-t^2}\, dt, \tag{37}$$

and the following shorthand has been introduced

$$A_+ = (\varepsilon_n^2+\Omega^2-\varepsilon_q^2)/2\varepsilon_n \quad , \quad A_- = (\varepsilon_n^2-\Omega^2+\varepsilon_q^2)/2\varepsilon_n$$
$$B_+ = (\varepsilon_n^2+\Omega^2-\varepsilon_p^2)/2\varepsilon_n \quad , \quad B_- = (\varepsilon_n^2-\Omega^2+\varepsilon_p^2)/2\varepsilon_n. \tag{38}$$

The singularity which appears in eq. (36) for $\varepsilon_p = \varepsilon_q$ can be easily dealt with by expanding the exponential and error functions. However, as this special case occurs again in the diagrams containing a self-energy insert, it will be presented there.

The result obtained from the contour integration of $I_{pq}^{m\Sigma}$ could now be recovered by integrating over z. However, we want to have a form in which the ultraviolet singularity is parametrized, and that results from inserting eq. (36) into (29) and first summing over the intermediate quarks and gluons. The divergence then appears as precisely the same non-integrable singularity in z as was found in the free-space diagram. Hence, $\mu_{\mathbf{a}}^{(2)}$ is given by

$$\mu_{\mathbf{a}}^{(2)} = g^2 \sum_{f'fc'c} \left\langle \hat{N} \left| \hat{a}^\dagger_{c'f'n} \left(\frac{\lambda^a}{2}\right)_{c'd} \left(\frac{\lambda^a}{2}\right)_{dc} Q\, \hat{a}_{cfn} \right| N \right\rangle \times \int_0^\infty dz \sum_{pqm\Sigma} g^{\Sigma\Sigma}\, \tilde{Q}_{np}^{m\Sigma}\, M_{pq}\, Q_{qn}^{m\Sigma}\, I_{pq}^{m\Sigma}(z). \tag{39}$$

3.3 Self-energy inserts

The remaining two divergent diagrams, which each have a self-energy insert on one of their external legs, are usually not included in cavity QCD calculations. The standard argument for discarding these diagrams is that the fields, masses, and charges appearing in the cavity QCD Lagrangian are renormalized quantities, and as such, already include self-energy effects [10]. However, as the order g^2 corrections to observables are not gauge-independent without these diagrams, we believe that they must be included to obtain a meaningful quantity. Furthermore, the finite parts of these diagrams do not vanish (in contrast to free-space field theory) and hence should have observable consequences. The result of the calculation of the vector coupling constant g_V also reassures us in that the self-energy diagrams should be retained, since the first-order correction vanishes when they are included, in accordance with

CVC. Finally, in the vertex diagram, the intermediate zero-energy scalar gluon (see Appendix C) has a divergent part which is exactly cancelled by a similar intermediate mode in the two diagrams with self-energy inserts.

Since the contributions to the magnetic moment from the two diagrams are equal, only the contribution $\mu_b^{(2)}$ from fig. 2(b) will be calculated here. As before, the gauge-independent part is given by

$$\mu_b^{(2)} = \lim_{\epsilon\to 0} g^2 \frac{3i\epsilon}{2}\frac{(-i)^3}{3!}\int d^4x_1 \int d^4x_2 \int d^4x_3\, e^{-\epsilon(|t_1|+|t_2|+|t_3|)} \tag{40}$$
$$\times \left\langle \hat{N}\middle| \left(\bar{\psi}(\vec{x}_1\times\vec{\gamma})_3 Q\psi\right)_{x_1} \left(\bar{\psi}\frac{\lambda_a}{2}\not{A}_a\psi\right)_{x_2} \left(\bar{\psi}\frac{\lambda_b}{2}\not{A}_b\psi\right)_{x_3} \middle|\hat{N}\right\rangle,$$

where the factor of $1/3!$ has been dropped since the $3!$ permutations of the co-ordinate labels are all equivalent. This immediately yields

$$\mu_b^{(2)} = \lim_{\epsilon\to 0}\frac{3i\epsilon}{2} g^2 \sum_{pqm\Sigma} g^{\Sigma\Sigma} M_{nq}\, \tilde{Q}_{qp}^{m\Sigma}\, Q_{pn}^{m\Sigma} \times \tag{41}$$
$$\int_{-\infty}^{\infty} dt_1\, dt_2\, dt_3 \int_{-\infty}^{\infty}\frac{d\omega}{2\pi}\frac{d\omega'}{2\pi}\frac{d\omega''}{2\pi}\frac{e^{-\epsilon(|t_1|+|t_2|+|t_3|)}\, e^{it_1(\varepsilon_1-\omega')}\, e^{it_2(\omega'-\omega''+\omega)}\, e^{it_3(\omega''-\omega-\varepsilon_2)}}{(\omega'-\varepsilon_q)(\omega''-\varepsilon_p)(\omega^2-\Omega^2)}.$$

Some care is needed when evaluating the time and ω integrals. Recall that, in free-space field theory, the Feynman amplitude for the divergent part of this graph was found to be ill-defined because the operator $(1/\not{p})\not{p}$ acting on a free-space spinor produces the undefined quantity 0/0. The ambiguity was only resolved by introducting adiabatic damping factors which are already included here.

One way of evaluating these integrals is to transform the damping factors into energy space using the Fourier transform

$$e^{-\epsilon|t|} = \int_{-\infty}^{\infty}\frac{dE}{2\pi}\frac{2\epsilon}{\epsilon^2+E^2}e^{iEt}. \tag{42}$$

With this transform, the integral becomes

$$\frac{3i\epsilon}{2}\int_{-\infty}^{\infty} dt_1\, dt_2\, dt_3 \int_{-\infty}^{\infty}\frac{d\omega}{2\pi}\frac{d\omega'}{2\pi}\frac{d\omega''}{2\pi}\frac{e^{-\epsilon(|t_1|+|t_2|+|t_3|)}\, e^{it_1(\varepsilon_{n'}-\omega')}\, e^{it_2(\omega'-\omega''+\omega)}\, e^{it_3(\omega''-\omega-\varepsilon_n)}}{(\omega'-\varepsilon_q)(\omega''-\varepsilon_p)(\omega^2-\Omega^2)}$$

$$= \frac{3i\epsilon}{2}\int_{-\infty}^{\infty}\frac{dE}{2\pi}\frac{dE'}{2\pi}\frac{dE''}{2\pi}\int_{-\infty}^{\infty} dt_1\, dt_2\, dt_3 \int_{-\infty}^{\infty}\frac{d\omega}{2\pi}\frac{d\omega'}{2\pi}\frac{d\omega''}{2\pi}$$
$$\frac{2\epsilon}{\epsilon^2+E^2}\frac{2\epsilon}{\epsilon^2+E'^2}\frac{2\epsilon}{\epsilon^2+E''^2}\frac{e^{it_1(\varepsilon_{n'}+E-\omega')}\, e^{it_2(\omega+\omega'+E'-\omega'')}\, e^{it_3(\omega''+E''-\omega-\varepsilon_n)}}{(\omega'-\varepsilon_q)(\omega''-\varepsilon_p)(\omega^2-\Omega^2)}$$

$$\underset{\epsilon\to 0}{=} \begin{cases} i\displaystyle\int\frac{d\omega}{2\pi}\frac{\delta(\varepsilon_n,\varepsilon_{n'})}{(\varepsilon_n-\varepsilon_q)(\omega+\varepsilon_{n'}-\varepsilon_p)(\omega^2-\Omega^2)} \equiv K_{pq}^{m\Sigma} & \text{if } \varepsilon_q\neq\varepsilon_n \\ -\dfrac{i}{2}\displaystyle\int\frac{d\omega}{2\pi}\frac{\delta(\varepsilon_n,\varepsilon_{n'})}{(\omega+\varepsilon_{n'}-\varepsilon_p)^2(\omega^2-\Omega^2)} \equiv I_{pp}^{m\Sigma} & \text{if } \varepsilon_q=\varepsilon_n \end{cases} \tag{43}$$

When the first case, $\varepsilon_q \neq \varepsilon_n$ in eq. (43), is inserted into eq. (41), we arrive for massless quarks at a finite self-energy contribution to the magnetic moment. The analogous result in free-space theory is zero. For massive quarks, this term diverges, and a counter-term must be introduced into the cavity Lagrangian to renormalize the mass [11]. However, here we shall restrict our attention to massless quarks. The second case, $\varepsilon_q = \varepsilon_n$, leads to a logarithmically divergent expression which is identical to that found in the free-space theory, eq. (16). This singularity, which in free-space field theory is equivalent to the charge renormalization constant, exactly cancels the divergence in the vertex correction diagram.

The remaining ω integral may now be evaluated in the standard way by Wick-rotating to Euclidean space and elevating the denominators into the exponent. Writing $K_{pq}^{m\Sigma} = \int_0^\infty dz\, K_{pq}^{m\Sigma}(z)$, we arrive at

$$K_{pq}^{m\Sigma}(z) = \frac{1}{4\varepsilon_n(\varepsilon_q-\varepsilon_n)\sqrt{\pi z}}\left(e^{-z\varepsilon_p^2}-e^{-z\Omega^2}\right)$$
$$+\frac{(\varepsilon_p+\varepsilon_n)^2-\Omega^2}{8\varepsilon_n^2(\varepsilon_q-\varepsilon_n)}\left[e^{zB_+^2-z\Omega^2}\operatorname{erf}\left(\sqrt{z}B_+\right)+e^{zB_-^2-z\varepsilon_p^2}\operatorname{erf}\left(\sqrt{z}B_-\right)\right] \tag{44}$$

for the first possibility in eq. (43). The quantities B_+ and B_- are defined in eq. (38). The other possibility, $I_{pp}^{m\Sigma} = \int_0^\infty dz\, I_{pp}^{m\Sigma}(z)$, is actually a special case of the inte-

gral (36) for the vertex correction diagram yielding

$$
\begin{aligned}
-I_{pp}^{m\Sigma}(z) = & \frac{1}{32\varepsilon_n^4\sqrt{\pi z}}\left[\left(\varepsilon_n+\varepsilon_p+\Omega\right)^2\left(\varepsilon_n+\varepsilon_p-\Omega\right)^2 z+2\varepsilon_n^2\right]e^{-z\Omega^2} \\
& + \frac{1}{32\varepsilon_n^4\sqrt{\pi z}}\left[\left((\varepsilon_n+\varepsilon_p)^2-\Omega^2\right)\left(\varepsilon_n^2-\varepsilon_p^2-2\varepsilon_n\varepsilon_p+\Omega^2\right)z+4\varepsilon_p\varepsilon_n^3 z-2\varepsilon_n^2\right]e^{-z\varepsilon_p^2} \\
& + \frac{1}{64\varepsilon_n^5}\left[\left(\varepsilon_n^2-\varepsilon_p^2+\Omega^2\right)\left((\varepsilon_n+\varepsilon_p)^2-\Omega^2\right)z-4\varepsilon_n^2\right]\left((\varepsilon_n+\varepsilon_p)^2-\Omega^2\right) \\
& \times\left[e^{-z\Omega^2}\,\mathrm{nerf}\left(\sqrt{z}B_+\right)+e^{-z\varepsilon_p^2}\,\mathrm{nerf}\left(\sqrt{z}B_-\right)\right]. \qquad (45)
\end{aligned}
$$

Inserting these integrals into eq. (41), we obtain for the vertex diagram containing a self-energy insert

$$
\mu_{\mathrm{b}}^{(2)} = g^2\int_0^\infty dz\sum_{pm\Sigma} g^{\Sigma\Sigma}\left(M_{nn}\,\tilde{Q}_{np}^{m\Sigma}\,Q_{pn}^{m\Sigma}I_{pp}^{m\Sigma}(z)+\sum_{q\neq n}M_{nq}\,\tilde{Q}_{qp}^{m\Sigma}\,Q_{pn}^{m\Sigma}K_{pq}^{m\Sigma}(z)\right). \qquad (46)
$$

3.4 Gauge-dependent terms

Recall that in free-space field theory, the sum of the three loop-diagrams contributing to the anomalous magnetic moment of the quark is gauge- independent, i.e. the terms containing the gauge parameter λ cancel identically. It will be shown here that this is also true in the cavity theory.

After subtracting the parts which do not depend on the gauge parameter, the remainder of the gluon propagator is given by (see appendix A)

$$
iD_{ab}^{\mu\nu}(x_1,x_2) = -i\delta_{ab}\frac{1-\lambda}{\lambda}\sum_{m\Sigma\Sigma'} a_{m\Sigma}^{\mu}(\vec{x}_1)\,a_{m\Sigma'}^{\nu\,*}(\vec{x}_2)\int\frac{d\omega}{2\pi}\frac{q^\Sigma q^{\Sigma'}}{q^4}e^{i\omega(t_2-t_1)}. \qquad (47)
$$

Substituting eq. (47) into eq. (26), the gauge-dependent part of the vertex correction diagram is found to be

$$
\mu_{\mathrm{a}}^{\lambda} = \lim_{\epsilon\to 0}\frac{3i\epsilon}{2}\frac{1-\lambda}{\lambda}g^2\sum_{pqm\Sigma\Sigma'}\tilde{Q}_{n'p}^{m\Sigma'}\,M_{pq}\,Q_{qn}^{m\Sigma}\,q^\Sigma q^{\Sigma'}\times \qquad (48)
$$

$$
\int_{-\infty}^{\infty}dt_1\,dt_2\,dt_3\int_{-\infty}^{\infty}\frac{d\omega}{2\pi}\frac{d\omega'}{2\pi}\frac{d\omega''}{2\pi}\frac{e^{-\epsilon(|t_1|+|t_2|+|t_3|)}\,e^{it_1(\varepsilon_{n'}+\omega-\omega')}\,e^{it_2(\omega'-\omega'')}\,e^{it_3(\omega''-\omega-\varepsilon_n)}}{(\omega'-\varepsilon_p)(\omega''-\varepsilon_q)(\omega^2-\Omega^2)^2},
$$

where the colour and flavour matrix elements have been omitted. From the definition of q^Σ in eq. (99), the sum over gluon polarizations is restricted to the scalar and

longitudinal modes only, and since the vertex integrals of these two polarizations are related by current conservation, eqs. (94) and (113), the sum over polarizations may be written in terms of scalar modes only

$$
\sum_{\Sigma\Sigma'}\tilde{Q}_{n'p}^{m\Sigma'}\,Q_{qn}^{m\Sigma}\,q^\Sigma q^{\Sigma'} = (\omega+\varepsilon_n-\varepsilon_q)(\omega+\varepsilon_{n'}-\varepsilon_p)\,\tilde{Q}_{n'p}^{m\mathcal{S}}\,Q_{qn}^{m\mathcal{S}}. \qquad (49)
$$

Evaluating the time and ω integrals as before, and inserting the polarization sum into eq. (48), we arrive at

$$
\mu_{\mathrm{a}}^{\lambda} = ig^2\frac{1-\lambda}{\lambda}\sum_{pqm}\tilde{Q}_{n'p}^{m\mathcal{S}}\,M_{pq}\,Q_{qn}^{m\mathcal{S}}\int_{-\infty}^{\infty}\frac{d\omega}{2\pi}\frac{\delta(\varepsilon_n,\varepsilon_{n'})}{(\omega^2-\Omega^2)^2}. \qquad (50)
$$

Finally, the remaining integral may easily be evaluated using standard techniques, yielding the gauge-dependent part of the vertex correction diagram

$$
\mu_{\mathrm{a}}^{\lambda} = -g^2\frac{1-\lambda}{\lambda}\int_0^\infty dz\sum_{pqm}\tilde{Q}_{np}^{m\mathcal{S}}\,M_{pq}\,Q_{qn}^{m\mathcal{S}}\sqrt{\frac{z}{4\pi}}\,e^{-z\Omega^2}. \qquad (51)
$$

In a similar way, the gauge-dependent part of the Feynman diagram with self-energy inserts, fig. 2(b), contributing to the quark's anomalous magnetic moment is found to be

$$
\mu_{\mathrm{b}}^{\lambda} = -g^2\frac{1-\lambda}{\lambda}\int_0^\infty dz\sqrt{\frac{z}{4\pi}}\,e^{-z\Omega^2}\sum_{pm}\left[\frac{1}{2}M_{nn}\,\tilde{Q}_{np}^{m\mathcal{S}}-\sum_{q\neq n}M_{nq}\,\tilde{Q}_{qp}^{m\mathcal{S}}\left(\frac{\varepsilon_q-\varepsilon_p}{\varepsilon_n-\varepsilon_q}\right)\right]Q_{pn}^{m\mathcal{S}}. \qquad (52)
$$

The sum $\mu_{\mathrm{a}}^{\lambda}+\mu_{\mathrm{b}}^{\lambda}+\mu_{\mathrm{c}}^{\lambda}$ can be evaluated numerically, and the result turns out to be exactly zero, which is what we expected from the free-space result.

3.5 One-gluon-exchange graphs

The remaining contributions to the baryon magnetic moments are the one-gluon-exchange diagrams, figs. 2(d)-(e). Only fig. 2(d) will be evaluated, since the two graphs have an equal contribution, given by

$$
\begin{aligned}
\mu_{\mathrm{d}}^{(2)} = & \lim_{\epsilon\to 0}g^2\frac{3i\epsilon}{2}\frac{(-i)^3}{3!}\int d^4x_1\int d^4x_2\int d^4x_3\,e^{-\epsilon(|t_1|+|t_2|+|t_3|)}\times \\
& \left\langle\hat{N}\middle|\left(\bar{\psi}\frac{\lambda_a}{2}\not{A}_a\psi\right)_{x_1}\left(\bar{\psi}\frac{\lambda_b}{2}\not{A}_b\psi\right)_{x_2}\left(\bar{\psi}\,(\vec{x}_3\times\vec{\gamma})_3 Q\,\psi\right)_{x_3}\middle|\hat{N}\right\rangle . \qquad (53)
\end{aligned}
$$

Inserting the quark and gluon propagators, and reducing the number of indices by writing the energy of the external quarks as ε_1 instead of ε_{n_1}, etc, the gauge-independent part of this expression becomes

$$\begin{aligned}\mu_{\rm d}^{(2)} &= \lim_{\epsilon\to 0} g^2 \frac{3\epsilon}{2} \sum_{c'f'cf} \left\langle \hat{N} \middle| \hat{a}^\dagger_{c'f'n_1} \hat{a}^\dagger_{d'g'n_3} \left(\frac{\lambda^a}{2}\right)_{c'c} \left(\frac{\lambda^a}{2}\right)_{d'd} Q\, \hat{a}_{cfn_2} \hat{a}_{dgn_4} \middle| \hat{N} \right\rangle \\ &\times \sum_{pm\Sigma} g^{\Sigma\Sigma}\, \tilde{Q}^{m\Sigma}_{n_1n_2}\, Q^{m\Sigma}_{n_3p}\, M_{pn_4} \int_{-\infty}^{\infty} dt_1\, dt_2\, dt_3 \\ &\times \int_{-\infty}^{\infty} \frac{d\omega}{2\pi} \frac{d\omega'}{2\pi} \frac{e^{-\epsilon(|t_1|+|t_2|+|t_3|)}\, e^{it_1(\varepsilon_1-\varepsilon_2+\omega)}\, e^{it_2(\varepsilon_3-\omega-\omega')}\, e^{it_3(\omega'-\varepsilon_4)}}{(\omega'-\varepsilon_p)(\omega^2-\Omega^2)}. \end{aligned} \tag{54}$$

A sum over all colours, flavours and cavity modes is understood in eq.(54). All the time and ω integrals can simply be evaluated to produce an energy denominator, since the one-gluon exchange diagrams are finite and do not need to be regularized. Omitting the tedious colour and flavour matrix element, this leads to

$$\mu_{\rm d}^{(2)} = g^2 \sum_{\substack{m\Sigma \\ p\neq n_4}} g^{\Sigma\Sigma}\, \tilde{Q}^{m\Sigma}_{n_1n_2}\, Q^{m\Sigma}_{n_3p}\, M_{pn_4} \frac{\delta(\varepsilon_1+\varepsilon_3\,,\,\varepsilon_2+\varepsilon_4)}{(\varepsilon_p-\varepsilon_4)\left[(\varepsilon_1-\varepsilon_2)^2-\Omega^2\right]}. \tag{55}$$

Since the virtual gluon in fig. 2(d) is coupled to a conserved quark current, labelled here by n_1n_2, one expects that this diagram will be independent of the gauge parameter. As is well-known from free-space QED, $q_\mu j^\mu = 0$ for a conserved current j^μ; hence the piece depending on the gauge parameter is zero. The relation analogous to this in cavity QCD can be written in terms of the polarization vector q_Σ as $q_\Sigma j^\Sigma = 0$, and consequently, the one-gluon exchange graphs are automatically gauge-independent in the cavity. This result can also be established directly.

We have used the magnetic moment operator as an example of how the nucleon observables can be calculated. The other observables are evaluated in exactly the same way, replacing the vertex integral for the magnetic moment operator with the appropriate vertex from those defined in appendix B.

4 Numerical results and discussion

We now turn to the evaluation of the expressions for the order α_s corrections to the nucleon observables which we have derived in the previous section. The sum over the spins of the intermediate quarks and gluon can easily be calculated analytically, leaving three infinite sums over the radial modes and two infinite sums over partial waves. The remaining partial wave sum is constrained by conservation of angular momentum and is thus finite. As these infinite sums are to be evaluated numerically, they must be truncated at some point, e.g. by including only cavity modes whose energy is less than a certain cut-off value $E_{\rm max}$.

The sum over vertex integrals, without the z-dependent terms, can be checked using the sum rules derived in appendix D, and the complete expressions for $\mathcal{O}^{(2)}$, as a function of z, can be compared with the free-space divergent terms. As we noted previously, the divergent parts of the free-space and cavity results should be the same. In order to compare them directly, the singular free-space function Λ^μ_S given by eq. (9) must be transformed from momentum to configuration space by sandwiching it between cavity spinors and integrating over the volume of the cavity. For example, the singular part of the anomalous magnetic moment in free space is given by

$$\mu_S = \alpha_s \int_0^\infty dz\, \mu_S(z) = \frac{\alpha_s}{4\pi} M_{n_1n_2} \int_0^\infty dz\, \frac{e^{-z}}{z} = \frac{2\alpha_s}{4\pi} M_{n_1n_2} \int_0^\infty dy\, \frac{e^{-y^2}}{y}. \tag{56}$$

It is convenient to shift the variable $z \to y^2$ here, since fig. 2(b) has a contribution from the self-energy which is finite for massless quarks (c.f. with the free-space theory, where the finite contribution is actually zero). However, the spectral function $\mu_{\rm b}^{(2)}(z)$ of this piece diverges as $z^{-1/2}$, i.e. it has an integrable singularity. Shifting the variable in the above manner transforms the divergent integrand $\mu_{\rm b}^{(2)}(z)$ into a function $\mu_{\rm b}^{(2)}(y)$ which is regular at the origin. This does not, of course, affect the other contribution from the charge renormalization constant, which is a non-integrable z^{-1} singularity.

The contribution from the vertex correction diagram is shown in upper frame of fig. 3, where the functions $\mu_{\rm a}^{(2)}(y)$ and $\mu_S(y)$ are plotted together against y on the same axes. The initial and final quark are both in the $1s_{\frac{1}{2}}\uparrow$ state, and the value of the energy cut-off used is $\Delta E_{\rm max} = 140$. The colour factor is not included. As expected, the nu-

merical calculation produces a curve which, for small y, lies exactly on the free-space divergent term. The lower frame of fig. 3 shows the finite remainder, after subtracting the free-space divergence from the cavity expression. In principle, the finite contribution of the vertex correction diagram to the anomalous magnetic moment (up to a finite renormalization) could be obtained by integrating this remainder.

Note that the function $\mu_a^{(2)}(y)$ has not been calculated all the way to zero on the y-axis. This is because the error introduced by truncating the infinite sum over cavity modes appears in the low y, or high energy region, creating a sharp kink. By using different values for the cut-off $E_{\max}$, one can establish that this point is at $y_{\min} \approx \pi/E_{\max}$. Apart from bringing the kink closer to the origin, increasing $E_{\max}$ has little other effect on the result. The 'missing' piece of $\mu_a^{(2)}(y)$ in the error region has been approximated by extrapolation using Chebychev polynomials.

Fig. 4 shows twice the contribution from the vertex diagram containing a self-energy insert on an external leg (the factor of two arises because there are two diagrams). Referring back to eq. (43), we see that this diagram has a finite 'self-energy' part, and a divergent charge renormalization part, which are plotted separately here. Also shown on the figure is the singular part of the free-space analogue of this diagram. Once again, the cavity and free-space functions exhibit precisely the same divergence. Clearly, when the vertex correction and self-energy insert diagrams are added, the divergences will cancel exactly.

The divergences from the loop diagrams have cancelled, but we are still confronted with the question of what, if any, finite renormalizations need to be applied. First of all, note that, apart from infrared problems, there is no finite renormalization of these diagrams in free space. This would appear to be the same in the cavity, at least for the observables generated by the conserved vector current.

It is well known that the vector coupling constant g_V, generated by the vector current, is not renormalized by the strong interaction. In the cavity, the sum of the $O(\alpha_s)$ corrections from the three loop-diagrams vanishes identically since the operator for g_V only connects diagonal states. This is easily seen from eqs. (23), (40) and (46). Furthermore, the two-body term also vanishes, leaving only the zero'th order result,

which has the required value of $g_V = 1$. Hence, no finite renormalization should be applied to the vector current.

The situation is less clear for g_A and $\langle r^2 \rangle_A$, since the axial vector current generating these observables is not conserved everywhere—it is discontinuous on the cavity surface. In view of this difficulty, we do not attempt to apply any *ad hoc* renormalization procedure, but note that possibility of a finite renormalization exists for the axial vector current.

The calculation of the one-gluon exchange diagrams does not present any problems since these are finite. The only point to note is that the contributions from the zero-energy scalar and longitudinal gluons must be calculated separately and added to the result. Once again, the sum rules provide powerful tests of the numerical algorithms. Restoring all factors of $\hbar$ and c and setting the cavity radius $R = 1$ fm, the results are given in table I. As a test, it is interesting to note that zeroth order and one-body part of the first order correction still respect the $SU(6)_{FS}$ relation $\mu_p/\mu_n = -\frac{3}{2}$, while the two-body part does not, as expected.

	0th order	1st order corrections			0th + 1st order		experiment
		1-body	2-body	total	$\alpha_s = 0.6$	$\alpha_s = 2.2$	[17]
μ_p	1.924	$-0.8034\alpha_s$	$0.0503\alpha_s$	$-0.7531\alpha_s$	1.472	0.267	2.793
μ_n	-1.282	$0.5356\alpha_s$	$0.0308\alpha_s$	$0.5664\alpha_s$	-0.942	-0.036	-1.913
$\langle r^2 \rangle_p$	0.5314	$-0.2598\alpha_s$	$-0.0147\alpha_s$	$-0.2745\alpha_s$	0.3667	-0.0725	0.69
$\langle r^2 \rangle_n$	0	0	$-0.0125\alpha_s$	$-0.0125\alpha_s$	-0.0075	-0.0275	-0.12
g_A	1.088	$0.2927\alpha_s$	$-0.0501\alpha_s$	$0.2426\alpha_s$	1.234	1.622	1.261
$\langle r^2 \rangle_A$	0.4979	$0.0104\alpha_s$	$-0.0441\alpha_s$	$-0.0337\alpha_s$	0.4777	0.4238	0.7

TABLE I:

Nucleon observables to order α_s for various values of α_s. The magnetic moments are in units of the nuclear magneton $\mu_N = e\hbar/2m_p$ and the radii in fm.

In the recent past, the calculation of the two-body corrections to nucleon observables has been presented in several papers [18, 19, 20, 21]. Høgaasen and Myhrer [21] clarified earlier calculations by Ushio [19] and Krivoruchenko [20] by evaluating the

contribution to $\mu^{(2)}$ due to the transverse magnetic gluon, to $\mu_p^{(2)} = 0$ for the proton, and $\mu_n^{(2)} = 0.133\,\mu_N$ for the neutron, using $\alpha_s = 2.2$ and $R = 5$ GeV^{-1}. These numbers are confirmed in the present calculation when the contribution from the scalar gluon is omitted. (The transverse electric and longitudinal gluons do not contribute anyway.) With the same parameters, Ushio finds the contribution from the transverse magnetic gluon to g_A to be 0.036, which we again can confirm. In his calculation, Ushio adds particular terms arising from the self-energy interaction to the contribution from the one-gluon-exchange. This is done to ensure that his Coulomb propagator satisfies the correct boundary conditions (see [1] for a discussion), and is not done here since the zero-energy scalar gluon mode takes care of that problem.

In calculating these corrections, Maxwell and Vento [10] use a similar formalism to that employed here which includes a rigorous treatment of the divergent vertex correction diagram. However, as the authors have not calculated the vertex diagrams containing self-energy inserts, their results for the one-body corrections are gauge-dependent, making a comparison with our results for these terms difficult, as these are performed in a different gauge. On the other hand, the one-gluon-exchange corrections are automatically gauge-independent, and can thus be compared with our calculation, shown in Table II. Here we have used $\alpha_s = 2.2$, which is equivalent to the $\alpha_c = 0.55$ used by Maxwell and Vento.

	Maxwell and Vento [10]	present paper
μ_p	−0.11	0.1107
μ_n	0.22	0.0678
$\langle r^2\rangle_p$	0.032	−0.0323
$\langle r^2\rangle_n$	−0.028	−0.0275
g_A	0.182	−0.1102
$\langle r^2\rangle_A$	0.124	−0.0970

TABLE II:

Comparison of results for the one-gluon-exchange of ref.[10] and the present paper

Our results for the one-gluon-exchange contribution agree with those from Maxwell and Vento [10] only in the case of the neutron charge squared radius, $\langle r^2\rangle_n$, with

differing signs being obtained for μ_p and $\langle r^2\rangle_p$. The agreement in the case of $\langle r^2\rangle_n$ suggests that the discrepancy could lie in the calculation of the zero-energy mode, since this is the only case for which the contribution from the zero-energy mode is zero.

In all of the nucleon observables investigated here, the $O(\alpha_s)$ corrections have made the agreement with experiment worse rather than better. The culprit is easily identified—it is those diagrams with self-energy inserts on the external legs, whose contributions may be divided into two parts for convenience. Firstly, there is a divergent part, equivalent to the free-space charge renormalization, which cancels the divergence from the vertex correction diagram, leaving a small finite remainder. Secondly, there is a part which is finite for massless quarks (the free-space analogue is zero). For massive quarks, this term also diverges, and would need to be cancelled by a mass renormalization counter-term [11]. It is found that the finite part is responsible for the large $O(\alpha_s)$ corrections, and it seems to have the 'wrong' sign. As mentioned earlier, the self-energy type diagrams are invariably dropped by other authors, but, as we have seen, there are compelling reasons for retaining them in the cavity. On the other hand, these results might be indicating that the boundary conditions confining the fields to the cavity are inadequate—a fact already hinted at by the disconcertingly large self-energies of a confined quark [7, 8] and gluon [12]. One should perhaps determine the boundary conditions in some self-consistent way such that the nucleon observables and self-energies have reasonable values, and this exercise may even lead to some insight into the mechanism of confinement. Alternatively, the poor fit of the calculated observables to the experimental values could be due in part to our omission of corrections such as the center-of-mass or effects of the pionic cloud at the cavity surface. It is also possible that higher-order diagrams should be included to obtain a better fit, and although that would be an extremely un-attractive task, it would be useful to know if the perturbative series really is converging.

We would like to thank Robert Lindebaum for useful comments. Financial support by the Foundation of Research Development is gratefully acknowledged.

Appendices

A Cavity modes and propagators

A.1 Quark cavity modes

The wave function of a quark with flavour f, mass m_f and energy ε_n is given by the solutions to the time-independent Dirac equation

$$\left(-i\vec{\gamma}\cdot\vec{\nabla}+m_f\right)u_n(\vec{r})=\varepsilon_n\gamma^0 u_n(\vec{r}) \tag{57}$$

subject to the boundary condition of the M.I.T. bag model [1] which, for a static, spherical cavity, reduces to

$$(i\vec{\gamma}\cdot\hat{r}+1)\,\hat{\psi}\Big|_{r=R}=0, \tag{58}$$

where R is the radius of the cavity. The solutions to the Dirac equation with this boundary condition are given by the spinors

$$u_n(\vec{r})=\begin{pmatrix} g_n(r)\chi^{\mu}_{\kappa}(\hat{r}) \\ i f_n(r)\chi^{\mu}_{-\kappa}(\hat{r})\end{pmatrix}. \tag{59}$$

The adjoint spinors are defined as

$$\bar{u}_n(\vec{r})=u_n^{\dagger}(\vec{r})\gamma^0. \tag{60}$$

Here, $n=\{\nu,\kappa,\mu\}$ labels the radial, Dirac and magnetic quantum numbers of the cavity mode, respectively, and $\chi^{\mu}_{\kappa}(\hat{r})$ is the usual two-component spherical spinor. The radial functions $g_n(r)$ and $f_n(r)$ are given by

$$g_n(r) = \frac{\mathcal{N}_n}{R^{3/2}}\,j_\ell(p_n r) \tag{61}$$

$$f_n(r) = \frac{\mathcal{N}_n}{R^{3/2}}\,\mathrm{sgn}(\kappa)\,\frac{p_n}{\varepsilon_n+m_f}\,j_{\bar{\ell}}(p_n r), \tag{62}$$

where $j_\ell(x)$ is the spherical Bessel function. The total and orbital angular momentum j and ℓ are defined in terms of the Dirac quantum number κ by

$$j(\kappa) = |\kappa|-\tfrac{1}{2} \tag{63}$$

$$\ell(\kappa) = j(\kappa)+\tfrac{1}{2}\,\mathrm{sgn}(\kappa) \tag{64}$$

$$\bar{\ell}(\kappa) = j(\kappa)-\tfrac{1}{2}\,\mathrm{sgn}(\kappa). \tag{65}$$

The momenta p_n are determined by the boundary condition, eq. (58), and are given by the solutions of the transcendental equation

$$j_\ell(x_n)+\frac{x_n}{\omega_n+\zeta_f}\,\mathrm{sgn}(\kappa)\,j_{\bar{\ell}}(x_n)=0, \tag{66}$$

where, for convenience, the energy, momentum and mass have been written in terms of the dimensionless quantities ω_n, x_n and ζ_f respectively. These are defined by

$$x_n = p_n R \tag{67}$$

$$\zeta_f = m_f R \tag{68}$$

$$\omega_n = \varepsilon_n R = \mathrm{sgn}(\nu)\sqrt[+]{x_n^2+\zeta_f^2}. \tag{69}$$

The positive and negative energy solutions are characterized by $\nu>0$ and $\nu<0$ respectively. These solutions are connected by the symmetry relation, $\varepsilon_{-\nu,\kappa}=-\varepsilon_{\nu,-\kappa}$. Finally, the normalization constant $\mathcal{N}_n$ is given by

$$\mathcal{N}_n^2=\frac{1}{2\omega_n(\omega_n+\kappa)+\zeta_f}\left(\frac{x_n}{j_\ell(x_n)}\right)^2. \tag{70}$$

The spinors (59) form a complete and orthonormal set of states defined within the cavity. Explicitly, the completeness relation is given by

$$\sum_n u_n(\vec{r})u_n^{\dagger}(\vec{r}\,')=\delta^{(3)}(\vec{r},\vec{r}\,')\,I, \tag{71}$$

where I is the unit 4×4 matrix, and the orthonormality by

$$\int d^3r\,u_n^{\dagger}(\vec{r})u_{n'}(\vec{r})=\delta_{nn'}. \tag{72}$$

A.2 Quark propagator

The quark field ψ may be expanded in the complete set of cavity modes

$$\hat{\psi}_{cf}(x)=\sum_{\substack{\kappa\mu\\ \nu>0}}\left[\hat{a}_{cfn}u_n(\vec{x})e^{-i\varepsilon_n t}+\hat{b}^{\dagger}_{cfn}u_{-n}(\vec{x})e^{i\varepsilon_n t}\right], \tag{73}$$

where the expansion coefficients $\hat{a}$ and $\hat{b}^{\dagger}$ are quark annihilation and antiquark creation operators respectively. The propagator is defined as the time-ordered product

of the fields

$$iS(x_1,x_2) = \left\langle \hat{0} \left| T\left[\hat{\psi}_{cf}(x_1)\hat{\bar{\psi}}_{c'f'}(x_2)\right] \right| \hat{0} \right\rangle \tag{74}$$

$$= \delta_{cc'}\,\delta_{ff'} \sum_{\substack{\kappa\mu \\ \nu>0}} \left[u_n(\vec{x}_1)\bar{u}_n(\vec{x}_2)\Theta(t_1-t_2) - u_{-n}(\vec{x}_1)\bar{u}_{-n}(\vec{x}_2)\Theta(t_2-t_1)\right] e^{-i\varepsilon_n|t_1-t_2|},$$

where the spinor indices have been suppressed. Using the integral representation of the theta function,

$$\Theta(t) = \lim_{\epsilon\to 0} -\frac{1}{2\pi i}\int_{-\infty}^{\infty} d\omega\, \frac{e^{-i\omega t}}{\omega + i\epsilon}, \tag{75}$$

the propagator may be written as

$$iS(x_1,x_2) = i\delta_{cc'}\,\delta_{ff'} \sum_n u_n(\vec{x}_1)\bar{u}_n(\vec{x}_2) \int \frac{d\omega}{2\pi}\, \frac{e^{-i\omega(t_1-t_2)}}{\omega - \varepsilon_n \pm i0}. \tag{76}$$

The sum over n now includes both positive and negative radial quantum numbers. The usual Feynman prescription for the poles should be employed when performing the contour integral, as indicated by the $\pm i0$. In other words, poles with positive energy are given a small, imaginary negative part while the negative energy poles acquire a positive imaginary part. Of course, the propagator is a Green's function of the Dirac equation

$$(i\partial\!\!\!/_x - m)\, S(x,y) = \delta^{(4)}(x,y)\ . \tag{77}$$

A.3 Gluon cavity modes

The gluon modes $a^{\mu}_{m\Sigma}(\vec{r})$ are solutions of the wave equation for massless vector fields

$$\left(\nabla^2 + \Omega_m^2\right) a^{\mu}_m(\vec{r}) = 0 \tag{78}$$

subject to the M.I.T. boundary conditions

$$\hat{r}\cdot\vec{\nabla} a^0_{m\mathcal{S}}(\vec{r})\Big|_{r=R} = 0 \tag{79}$$

$$\hat{r}\cdot\vec{a}_{m\Sigma}(\vec{r})\Big|_{r=R} = \hat{r}\times\left(\vec{\nabla}\times\vec{a}_{m\Sigma}(\vec{r})\right)\Big|_{r=R} = 0 \qquad \Sigma = \mathcal{L},\mathcal{M},\mathcal{E}. \tag{80}$$

The solutions of these equations are labelled by $\Sigma = \mathcal{S},\mathcal{L},\mathcal{M},\mathcal{E}$ for the scalar, longitudinal, magnetic and electric polarizations, respectively, and $m = \{N, J, M\}$ denotes

the radial, total angular momentum and magnetic quantum numbers, respectively. In terms of spherical Bessel functions and vector spherical harmonics, the cavity modes are

$$a^0_{m\mathcal{S}}(\vec{r}) = \frac{\mathcal{N}_{m\mathcal{S}}}{R^{3/2}}\, i j_J(\Omega^{\mathcal{S}}_m r)\, Y_{JM}(\hat{r}) \tag{81}$$

$$\vec{a}_{m\mathcal{L}}(\vec{r}) = \frac{\mathcal{N}_{m\mathcal{L}}}{\sqrt{R^3(2J+1)}}\left[\sqrt{J}\, j_{J-1}(\Omega^{\mathcal{L}}_m r)\,\vec{Y}^{J-1}_{JM}(\hat{r}) + \sqrt{J+1}\, j_{J+1}(\Omega^{\mathcal{L}}_m r)\,\vec{Y}^{J+1}_{JM}(\hat{r})\right] \tag{82}$$

$$\vec{a}_{m\mathcal{M}}(\vec{r}) = \frac{\mathcal{N}_{m\mathcal{M}}}{R^{3/2}}\, j_J(\Omega^{\mathcal{M}}_m r)\,\vec{Y}^{J}_{JM}(\hat{r}) \tag{83}$$

$$\vec{a}_{m\mathcal{E}}(\vec{r}) = \frac{\mathcal{N}_{m\mathcal{E}}}{\sqrt{R^3(2J+1)}}\left[\sqrt{J+1}\, j_{J-1}(\Omega^{\mathcal{E}}_m r)\,\vec{Y}^{J-1}_{JM}(\hat{r}) - \sqrt{J}\, j_{J+1}(\Omega^{\mathcal{E}}_m r)\,\vec{Y}^{J+1}_{JM}(\hat{r})\right], \tag{84}$$

where Ω^{Σ}_m is the energy of the m'th mode with polarization Σ. The total angular momentum J is defined such that $J \geq 0$ for $\Sigma = \mathcal{S},\mathcal{L}$ and $J \geq 1$ for $\Sigma = \mathcal{M},\mathcal{E}$. The boundary conditions for a spherical cavity reduce to the following eigenvalue conditions for the gluon energy

$$\begin{aligned} J j_J(\Omega^{\Sigma}_m R) - \Omega^{\Sigma}_m R\, j_{J+1}(\Omega^{\Sigma}_m R) &= 0 \qquad & \Sigma = \mathcal{S},\,\mathcal{L} \\ (J+1)\, j_J(\Omega^{\mathcal{M}}_m R) - \Omega^{\mathcal{M}}_m R\, j_{J+1}(\Omega^{\mathcal{M}}_m R) &= 0 \qquad & \Sigma = \mathcal{M} \\ j_J(\Omega^{\mathcal{E}}_m R) &= 0 \qquad & \Sigma = \mathcal{E}. \end{aligned} \tag{85}$$

The normalization constants are given by

$$\mathcal{N}^{-2}_{m\mathcal{S}} = \mathcal{N}^{-2}_{m\mathcal{L}} = \tfrac{1}{2}\, j_J^2(\Omega^{\mathcal{S}}_m R)\left[1 - \frac{J(J+1)}{(\Omega^{\mathcal{S}}_m R)^2}\right] \tag{86}$$

$$\mathcal{N}^{-2}_{m\mathcal{M}} = \tfrac{1}{2}\, j_J^2(\Omega^{\mathcal{M}}_m R)\left[1 - \frac{J(J+1)}{(\Omega^{\mathcal{M}}_m R)^2}\right] \tag{87}$$

$$\mathcal{N}^{-2}_{m\mathcal{E}} = \tfrac{1}{2}\, j_{J+1}^2(\Omega^{\mathcal{E}}_m R). \tag{88}$$

The set of gluon modes satisfying eq. (78) is complete and orthonormal. These properties are most conveniently expressed by introducing the metric tensor in polarization space, $g^{\Sigma\Sigma}$. With its help, the completeness relation may be written as

$$\sum_{m\Sigma} g^{\Sigma\Sigma}\, a^{\mu}_{m\Sigma}(\vec{r})\, a^{\nu *}_{m\Sigma}(\vec{r}\,') = g^{\mu\nu}\,\delta^{(3)}(\vec{r},\vec{r}\,'), \tag{89}$$

and orthonormality is then given by

$$\int d^3r\, g_{\mu\nu}\, a^{\mu}_{m\Sigma}(\vec{r})\, a^{\nu *}_{m'\Sigma'}(\vec{r}) = g^{\Sigma\Sigma'}\delta_{mm'}. \tag{90}$$

The diagonal metric $g^{\Sigma\Sigma}$ is represented as

$$g^{\mathcal{S}\mathcal{S}} = -g^{\mathcal{L}\mathcal{L}} = -g^{\mathcal{M}\mathcal{M}} = -g^{\mathcal{E}\mathcal{E}} = 1, \qquad g^{\Sigma\Sigma'} = 0 \quad \text{if } \Sigma \neq \Sigma'. \tag{91}$$

Finally, a few useful identities concerning the cavity modes are noted. Using the properties of the vector spherical harmonics, the complex conjugate of $a^{\mu}_{m\Sigma}(\vec{r})$ is

$$a^{\mu *}_{m\Sigma}(\vec{r}) = (-1)^M \eta^{\Sigma} a^{\mu}_{m^*\Sigma}(\vec{r}) \tag{92}$$

with the definition $m^* = \{N, J, -M\}$. The phase η^{Σ} is shorthand for

$$\eta^{\Sigma} = \begin{cases} -1 & \text{if } \Sigma = \mathcal{S}, \mathcal{M} \\ +1 & \text{if } \Sigma = \mathcal{L}, \mathcal{E}. \end{cases} \tag{93}$$

The scalar and longitudinal modes are related by current conservation i.e.

$$a^{0}_{m\mathcal{S}}(\vec{r}) = -\frac{i}{\Omega^{\mathcal{S}}_m}\vec{\nabla}\cdot\vec{a}_{m\mathcal{L}}(\vec{r}) \tag{94}$$

$$\vec{a}_{m\mathcal{L}}(\vec{r}) = -\frac{i}{\Omega^{\mathcal{S}}_m}\vec{\nabla} a^{0}_{m\mathcal{S}}(\vec{r}). \tag{95}$$

A.4 Gluon propagator

The gluon field may be expanded in the complete set of cavity modes

$$\hat{A}^{\mu}_a(x) = \sum_{m\Sigma} \frac{1}{\sqrt{2\Omega^{\Sigma}_m}} \left[\hat{c}^{\Sigma}_{am} a^{\mu}_{m\Sigma}(\vec{x}) e^{-i\Omega^{\Sigma}_m t} + \hat{c}^{\Sigma\dagger}_{am} a^{\mu *}_{m\Sigma}(\vec{x}) e^{i\Omega^{\Sigma}_m t} \right]. \tag{96}$$

The propagator in the Feynman gauge ($\lambda = 1$) is given by

$$\begin{aligned} iD^{\mu\nu}_{ab}(x_1, x_2) &= \left\langle \hat{0} \left| T\left\{ \hat{A}^{\mu}_a(x_1) \hat{A}^{\nu}_b(x_2) \right\} \right| \hat{0} \right\rangle \\ &= -\delta_{ab} \sum_{m\Sigma} \frac{g^{\Sigma\Sigma}}{2\Omega^{\Sigma}_m} a^{\mu}_{m\Sigma}(\vec{x}_1) a^{\nu *}_{m\Sigma}(\vec{x}_2)\, e^{-i\Omega^{\Sigma}_m |t_1 - t_2|}. \end{aligned} \tag{97}$$

Using the integral representation of $\Theta(t)$, eq. (75), the propagator may be written as

$$iD^{\mu\nu}_{ab}(x_1, x_2) = -i\delta_{ab} \sum_{m\Sigma} g^{\Sigma\Sigma}\, a^{\mu}_{m\Sigma}(\vec{x}_1) a^{\nu *}_{m\Sigma}(\vec{x}_2) \int \frac{d\omega}{2\pi} \frac{e^{i\omega(t_2 - t_1)}}{q^2 + i0}, \tag{98}$$

where the vector q^{Σ} in polarization space has been introduced. This vector is defined as

$$\begin{aligned} q^{\Sigma} &\equiv (q^{\mathcal{S}}, q^{\mathcal{L}}, q^{\mathcal{M}}, q^{\mathcal{E}}) = (\omega, \Omega^{\Sigma}_m, 0, 0) \\ q_{\Sigma} &= (\omega, -\Omega^{\Sigma}_m, 0, 0), \end{aligned} \tag{99}$$

and satisfies the condition $q^2 = \omega^2 - (\Omega^{\Sigma}_m)^2$. The functions $D^{\mu\nu}_{ab}(x, y)$ satisfy the inhomogenous d'Alembert equations

$$\Box_x D^{\mu\nu}_{ab}(x, y) = \delta_{ab}\, g^{\mu\nu}\, \delta^{(4)}(x, y). \tag{100}$$

More generally, the gluon propagator in an arbitrary covariant gauge is given by [24]

$$iD^{\mu\nu}_{ab}(x_1, x_2) = i\delta_{ab} \sum_{m\Sigma\Sigma'} a^{\mu}_{m\Sigma}(\vec{x}_1) a^{\nu *}_{m\Sigma'}(\vec{x}_2) \int \frac{d\omega}{2\pi} \left[\frac{-g^{\Sigma\Sigma'}}{q^2} - \frac{1-\lambda}{\lambda} \frac{q^{\Sigma} q^{\Sigma'}}{q^4} \right] e^{i\omega(t_2 - t_1)}. \tag{101}$$

B Vertex integrals

B.1 Quark-gluon vertex integral

The interaction between quarks and gluons is described by the integral which is defined as

$$Q^{m\Sigma}_{nn'} = i \int d^3r\, \bar{u}_n(\vec{r})\gamma_\mu u_{n'}(\vec{r})\, a^\mu_{m\Sigma}(\vec{r}). \tag{102}$$

Closely associated with this integral is one in which the gluon field is replaced with its complex conjugate, which will be written as

$$\tilde{Q}^{m\Sigma}_{nn'} = i \int d^3r\, \bar{u}_n(\vec{r})\gamma_\mu u_{n'}(\vec{r})\, a^{\mu *}_{m\Sigma}(\vec{r}). \tag{103}$$

Using (92), this may be reduced to (102) as

$$\tilde{Q}^{m\Sigma}_{nn'} = (-1)^M \eta^\Sigma i \int d^3r\, \bar{u}_n(\vec{r})\gamma_\mu u_{n'}(\vec{r})\, a^\mu_{m^*\Sigma}(\vec{r}) = (-1)^M \eta^\Sigma Q^{m^*\Sigma}_{nn'} = -Q^{m\Sigma}_{n'n}. \tag{104}$$

Following ref. [22], but using a slightly different notation, the radial and angular dependence of (102) can be separated as

$$\begin{aligned} Q^{m\Sigma}_{nn'} &= R^{-3/2} R^{m\Sigma}_{nn'} \int d\Omega\, \chi^{\mu\dagger}_\kappa(\hat{r}) Y_{JM}(\hat{r}) \chi^{\mu'}_{\kappa'}(\hat{r}) \qquad \Sigma = \mathcal{S}, \mathcal{L}, \mathcal{E} \\ Q^{m\mathcal{M}}_{nn'} &= R^{-3/2} R^{m\mathcal{M}}_{nn'} \int d\Omega\, \chi^{\mu\dagger}_\kappa(\hat{r}) Y_{JM}(\hat{r}) \chi^{\mu'}_{-\kappa'}(\hat{r}) \qquad \Sigma = \mathcal{M}. \end{aligned} \tag{105}$$

The integral over the angular variables is readily evaluated by expanding the spinors and spherical harmonics in a Clebsch-Gordan series. In terms of the Wigner $3j$-symbols, the result is

$$\begin{aligned} \int d\hat{r}\, \chi^{\mu\dagger}_\kappa(\hat{r}) Y_{JM}(\hat{r}) \chi^{\mu'}_{\kappa'}(\hat{r}) &= \frac{(-1)^{\mu+1/2}}{\sqrt{4\pi}} \frac{1+(-1)^{\ell+J+\ell'}}{2} \hat{j}\hat{J}\hat{j}' \\ &\quad \times \begin{pmatrix} j & J & j' \\ -\mu & M & \mu' \end{pmatrix} \begin{pmatrix} j & J & j' \\ \frac{1}{2} & 0 & -\frac{1}{2} \end{pmatrix}, \end{aligned} \tag{106}$$

where the abbreviation $\hat{J} = \sqrt{2J+1}$ has been introduced. The notation for the $3j$-symbols is that of the encyclopedic Varshalovich *et al.* [25], and is consistent with the standard notation of Edmonds [26]. The radial integrals are given by

$$R^{m\mathcal{S}}_{nn'} = -\mathcal{N}_{m\mathcal{S}} \int_0^R dr\, r^2\, j_J(\Omega^{\mathcal{S}}_m r) S_{nn'}(r) \tag{107}$$

$$\begin{aligned} R^{m\mathcal{L}}_{nn'} = -\frac{\mathcal{N}_{m\mathcal{S}}}{\Omega^{\mathcal{S}}_m} \int_0^R dr\, r \Big\{ &\Big[\Omega^{\mathcal{S}}_m r\, j_{J+1}(\Omega^{\mathcal{S}}_m r) - J j_J(\Omega^{\mathcal{S}}_m r)\Big] U_{nn'}(r) \\ &+ (\kappa - \kappa')\, j_J(\Omega^{\mathcal{S}}_m r) T_{nn'}(r) \Big\} \end{aligned} \tag{108}$$

$$R^{m\mathcal{M}}_{nn'} = \frac{\kappa + \kappa'}{\sqrt{J(J+1)}} \mathcal{N}_{m\mathcal{M}} \int_0^R dr\, r^2\, j_J(\Omega^{\mathcal{M}}_m r) T_{nn'}(r) \tag{109}$$

$$\begin{aligned} R^{m\mathcal{E}}_{nn'} = \frac{\mathcal{N}_{m\mathcal{E}}}{\Omega^{\mathcal{E}}_m \sqrt{J(J+1)}} \int_0^R dr\, r \Big\{ &J(J+1)\, j_J(\Omega^{\mathcal{E}}_m r) U_{nn'}(r) \\ &+ (\kappa - \kappa') \Big[J j_J(\Omega^{\mathcal{E}}_m r) - \Omega^{\mathcal{E}}_m r\, j_{J-1}(\Omega^{\mathcal{E}}_m r) \Big] T_{nn'}(r) \Big\}. \end{aligned} \tag{110}$$

Three further abbreviations have been introduced here for the radial parts of the quark wave functions. They are

$$\begin{aligned} S_{nn'} &= g_n g_{n'} + f_n f_{n'} \\ T_{nn'} &= g_n f_{n'} + f_n g_{n'} \\ U_{nn'} &= g_n f_{n'} - f_n g_{n'}. \end{aligned} \tag{111}$$

It is convenient to include the phase factor from the angular integration of eq. (106), which contains the parity selection rule, into the radial functions by defining

$$S^{m\Sigma}_{nn'} = \frac{1 - g^{\Sigma\Sigma} \eta_\Sigma (-1)^{\ell+J+\ell'}}{2} R^{m\Sigma}_{nn'}. \tag{112}$$

The vertex integrals involving the scalar and longitudinal modes are related by current conservation,

$$Q^{m\mathcal{L}}_{nn'} = \frac{\varepsilon_{n'} - \varepsilon_n}{\Omega^{\mathcal{S}}_m} Q^{m\mathcal{S}}_{nn'}. \tag{113}$$

The angular integrals for the quark-quark-gluon vertex are easily evaluated, while the radial integrals require lengthy numerical calculation.

B.2 Magnetic moment vertex

The interaction between quarks and the magnetic moment operator is defined by the integral

$$M_{nn'} = \frac{1}{2}\int d^3r\, \bar{u}_n(\vec{r})\Big(\vec{r}\times\vec{\gamma}\Big)_z u_{n'}(\vec{r}). \tag{114}$$

The radial and angular dependence in eq. (114) may be separated yielding

$$M_{nn'} = -(\kappa+\kappa')A_{\kappa\kappa'}\int_0^R dr\, r^3\Big(g_n f_{n'} + f_n g_{n'}\Big), \tag{115}$$

where the angular integral has been defined as

$$A_{\kappa\kappa'} \equiv \sqrt{\frac{\pi}{3}}\int d\hat{r}\, \chi_\kappa^{\mu\dagger}(\hat{r})Y_{10}(\hat{r})\chi_{-\kappa'}^{\mu'}(\hat{r}). \tag{116}$$

Evaluating the angular integral explicitly yields

$$-A_{\kappa\kappa'} = \begin{cases} \dfrac{\mu}{4\kappa^2-1}\delta_{\mu\mu'} & \text{if } \kappa'=\kappa \\[2ex] \dfrac{\sqrt{(|\kappa|+\frac{1}{2})^2-\mu^2}}{4|\kappa|+2}\delta_{\mu\mu'} & \text{if } \kappa'=-\kappa\pm 1, \end{cases} \tag{117}$$

where $A_{\kappa\kappa'}$ is symmetric. All other possibilities are zero. The radial matrix elements of eq. (115) reduce to

$$\int_0^R dr\, r^3\Big(g_n f_{n'} + f_n g_{n'}\Big) = \tag{118}$$

$$= \begin{cases} \dfrac{R}{2}\dfrac{4\omega\kappa - 2\zeta + 4\kappa^2 - 1}{2\omega(\omega+\kappa)+\zeta} & \kappa'=\kappa\,,\ \nu'=\nu \\[2ex] \dfrac{-2xx'R\times\phi}{(\omega+\omega')^2\sqrt{[2\omega(\omega+\kappa)+\zeta][2\omega'(\omega'+\kappa)+\zeta]}} & \kappa'=\kappa\,,\ \nu'\neq\nu \\[2ex] \dfrac{-2xx'R(\omega-\omega'+\kappa-\kappa')\times\phi}{(\omega+\omega')(x^2-x'^2)\sqrt{[2\omega(\omega+\kappa)+\zeta][2\omega'(\omega'+\kappa')+\zeta]}} & \kappa'=-\kappa\pm 1. \end{cases}$$

Here, the dimensionless energy, momentum and mass variables, introduced in equation (67) to (69) of appendix A, are being used, and the notation is such that $\omega' \equiv \omega_{n'}$ and $x' \equiv x_{n'}$. The factor ϕ is a phase factor given by

$$\phi = (-1)^{\rho+\rho'}\ , \qquad \rho = \begin{cases} |\nu|+1 & \kappa<0,\ \nu<0 \\ |\nu| & \text{otherwise.} \end{cases} \tag{119}$$

B.3 Charge radius vertex

The vertex integral of electromagnetic charge radius is given by

$$P_{nn'} = \int d^3r\, |\vec{r}|^2\, u_n^+(\vec{r})u_{n'}(\vec{r}). \tag{120}$$

This is easily separated, and the trivial angular integral evaluated immediately to give

$$P_{nn'} = \int_0^R dr\, r^4\Big(g_n g_{n'} + f_n f_{n'}\Big)\delta_{\kappa\kappa'}\delta_{\mu\mu'}. \tag{121}$$

Evaluating the radial integral yields

$$P_{\nu\nu'} = \begin{cases} \dfrac{\Big[(2\omega^2+2\omega\kappa+3\zeta)(4\kappa^2-1+2x^2)+4\zeta(2\omega\kappa-\zeta)+2x^2\Big]R^2}{6x^2(2\omega^2+2\omega\kappa+\zeta)} & \text{if } \nu'=\nu \\[2ex] \dfrac{4xx'R^2\Big[(\omega+\omega')(\omega+\omega'+2\kappa)+2\zeta\Big]\times\phi}{(x^2-x'^2)^2\sqrt{[2\omega(\omega+\kappa)+\zeta][2\omega'(\omega'+\kappa)+\zeta]}} & \text{if } \nu'\neq\nu, \end{cases} \tag{122}$$

where the phase factor ϕ was defined in eq. (119).

B.4 Axial vector vertex

The integral arising from the axial vector coupling constant is defined by

$$G_{nn'} = \int d^3r\, \bar{u}_n(\vec{r})\,\gamma_z\gamma_5\, u_{n'}(\vec{r}) = \int d^3r\, u_n^\dagger(\vec{r})\sigma_z u_{n'}(\vec{r}). \tag{123}$$

After separating the angular and radial dependence, and evaluating the angular integral, this expression becomes

$$G_{nn'} = 2A_{\kappa\kappa'}\int_0^R dr\, r^2\Big[(\kappa+\kappa')(g_n g_{n'} - f_n f_{n'}) - g_n g_{n'} - f_n f_{n'}\Big], \tag{124}$$

where $A_{\kappa\kappa'}$ was defined in eq. (117). For all possible quantum numbers nn', the remaining integral is given by

$$\int_0^R dr\, r^2\Big[(\kappa+\kappa')(g_n g_{n'} - f_n f_{n'}) - g_n g_{n'} - f_n f_{n'}\Big] = \tag{125}$$

$$= \begin{cases} \dfrac{\zeta(4\kappa^2-1)+2\omega(2\kappa\zeta-\omega)}{2\omega(\omega+\kappa)+\zeta} & \kappa'=\kappa\,,\ \ \nu'=\nu \\[2ex] \dfrac{4\kappa x x' \times \phi}{(\omega+\omega')\sqrt{[2\omega(\omega+\kappa)+\zeta][2\omega'(\omega'+\kappa)+\zeta]}} & \kappa'=\kappa\,,\ \ \nu'\neq\nu \\[2ex] \dfrac{\pm 2xx'(\omega-\omega'+\kappa-\kappa')\times\phi}{(x^2-x'^2)\sqrt{[2\omega(\omega+\kappa)+\zeta][2\omega'(\omega'+\kappa')+\zeta]}} & \kappa'=-\kappa\pm 1. \end{cases}$$

B.5 Axial charge radius vertex

The integral for this operator is similar to that arising from the axial vector coupling constant, the only difference being the power to which r is raised in the radial integral. Hence, only the radial integral need be evaluated here.

$$\int_0^R dr\, r^4\Big[(\kappa+\kappa')(g_n g_{n'} - f_n f_{n'}) - g_n g_{n'} - f_n f_{n'}\Big] = I \tag{126}$$

Case 1: $\kappa'=\kappa,\ \nu'=\nu$

$$I = R^2\Big[\Big\{2\omega^2+2(\zeta+1)(x^2+2\kappa\omega)+\zeta(4\kappa^2-3)\Big\}(4\kappa^2-1)+4x^2(\zeta+1)(2\kappa\omega-1)$$
$$+4\omega(2\omega-x^2\omega-4\kappa\zeta)\Big]\Big/6x^2(2\omega^2+2\omega\kappa+\zeta)$$

Case 2: $\kappa'=\kappa,\ \nu'\neq\nu$

$$I = \frac{4xx'R^2\Big[\kappa(x^2-x'^2)^2-4\kappa(x^2+x'^2)+(\omega+\omega')^2(4\zeta\kappa-\omega-\omega')+2\zeta(\omega+\omega')(4\kappa^2-1)\Big]}{(\omega+\omega')^3(\omega-\omega')^2\sqrt{[2\omega(\omega+\kappa)+\zeta][2\omega'(\omega'+\kappa)+\zeta]}}$$

Case 3: $\kappa'=-\kappa+1$

$$I = 2xx'R^2\Big[\Big\{(\omega-\omega'+\kappa-\kappa')(x^2-x'^2+2\kappa-2\kappa')+2(\omega+\omega')(2\zeta-\omega-\omega')\Big\}(x^2-x'^2)$$
$$-4(x^2+x'^2)(\omega-\omega'+\kappa-\kappa')\Big]\Big/(x^2-x'^2)^3\sqrt{[2\omega(\omega+\kappa)+\zeta][2\omega'(\omega'+\kappa')+\zeta]}.$$

Case 4: $\kappa'=-\kappa-1$

$$I = -2xx'R^2\Big[\Big\{(\omega-\omega'+\kappa-\kappa')(x^2-x'^2-2\kappa+2\kappa')+2(\omega+\omega')(2\zeta+\omega+\omega')\Big\}(x^2-x'^2)$$
$$-4(x^2+x'^2)(\omega-\omega'+\kappa-\kappa')\Big]\Big/(x^2-x'^2)^3\sqrt{[2\omega(\omega+\kappa)+\zeta][2\omega'(\omega'+\kappa')+\zeta]}.$$

C Zero-energy scalar mode

For the scalar gluon, the M.I.T. boundary conditions yield the eigenvalue equation

$$\frac{d}{dr} j_J(\Omega_m^S r)\Big|_{r=R} = 0 \tag{127}$$

which has a solution $\Omega_{m_0}^S = 0$ for $m_0 \equiv \{N, J, M\} = \{0, 0, 0\}$. This solution must be included in order to obtain a complete set of modes, and to be able to construct a propagator that is consistent with the boundary condition [6, 13, 27]. The normalized gluon mode corresponding to this solution is

$$a_{m_0 S}^0 = i\sqrt{\frac{3}{4\pi}}. \tag{128}$$

As $\Omega_{m_0}^S$ appears in the denominator of eqs.(96) and (97), the corresponding quantities are infinite. One way of dealing with this problem is to perform the calculations for a mode with the same quantum numbers, but with a small non-zero energy $\Omega_{m_0}^S \neq 0$, taking the limit $\Omega_{m_0}^S \to 0$ at the end of the calculation. This method works, but is not entirely satisfactory, as one obtains terms which diverge like Ω^{-1}, and one ignores the instantaneous nature of such a zero-energy mode.

A more consistent approach is to examine the scalar part of the gluon propagator more carefully. Ignoring the zero-energy modes, the Coulomb part of the propagator can be written as the sum over the scalar and longitudinal modes

$$D_{ab}^{00}(x, x') = -\delta_{ab} \sum_{\Sigma=S,\mathcal{L}} g^{\Sigma\Sigma} a_{m\Sigma}^0(\vec{x}) a_{m\Sigma}^{0*}(\vec{x}') \int \frac{d\omega}{2\pi} \frac{e^{-i\omega(t-t')}}{\omega^2 - \Omega^2 + i0}. \tag{129}$$

It is important to note that the propagator is always sandwiched between conserved currents, i.e.

$$\partial_\mu j^\mu = \partial_0 \rho + \vec{\nabla} \cdot \vec{j} = 0. \tag{130}$$

Thus, what we usually evaluate are integrals of the form

$$A = \int d^4x j_\mu(x) \left(a_{mS}^\mu(\vec{x}) e^{-i\omega t} - a_{m\mathcal{L}}^\mu(\vec{x}) e^{-i\omega t} \right). \tag{131}$$

Using $\vec{a}_{m\mathcal{L}}(\vec{x}) = -(i/\Omega)\vec{\nabla} a_{mS}^0(\vec{x})$ and performing two partial integrations, one finds

$$A = (1 + \frac{\omega}{\Omega}) \int d^4x \rho(x) a_{mS}^0(\vec{x}) e^{-i\omega t}. \tag{132}$$

Thus the Coulomb (i.e. scalar plus longitudinal) part of the propagator can be written as

$$\begin{aligned} D_C^{\mu\nu}(x, x') &= \delta^{\mu 0}\delta^{\nu 0} \int \frac{d\omega}{2\pi} e^{-i\omega(t-t')} \sum_m \frac{a_{mS}^0(\vec{x}) a_{mS}^{0*}(\vec{x}')}{\Omega^2} \\ &= \delta^{\mu 0}\delta^{\nu 0}\delta(t-t') \sum_m \frac{a_{mS}^0(\vec{x}) a_{mS}^0(\vec{x}')}{\Omega^2} \\ &= \delta^{\mu 0}\delta^{\nu 0}\delta(t-t') G(\vec{x}, \vec{x}'). \end{aligned} \tag{133}$$

One can see by substitution that this Green's function satisfies

$$\nabla^2 G(\vec{x}, \vec{x}') = -\sum_m a_{mS}^0(\vec{x}) a_{mS}^{0*}(\vec{x}') \tag{134}$$

which would yield a delta function, if the sum on the right-hand side of eq.(134) included the zero-energy mode. However, it is not possible to include the mode m_0 in eq. (129). The contribution of the zero energy mode to the propagator is given by

$$\nabla^2 G_0(\vec{x}, \vec{x}') = -\frac{3}{4\pi}. \tag{135}$$

Hence by integrating and using the symmetry of the propagator, we arrive at

$$G_0(x, x') = \frac{1}{4\pi}\left(c - \frac{r^2}{2} - \frac{r'^2}{2}\right), \tag{136}$$

where c is an arbitrary constant. Thus the contribution of this mode to the full propagator is

$$D_0^{\mu\nu}(x, x') = \delta^{\mu 0}\delta^{\nu 0}\delta(t-t')\frac{1}{4\pi}\left(c - \frac{r^2}{2} - \frac{r'^2}{2}\right). \tag{137}$$

The presence of the arbitary constant is not a problem, as it does not contribute to any diagram we have calculated. If one excludes the zero-energy mode [24], the Coulomb part of the propagator in the Feynman gauge differs from that in the Coulomb gauge by

$$\delta G(x, x') = \frac{1}{4\pi}\left(\frac{9}{5} - \frac{r^2}{2} - \frac{r'^2}{2}\right). \tag{138}$$

Thus one could use $c = 9/5$ to get results in agreement with the Coulomb gauge; one would simply have to insert

$$D^{\mu\nu}(x, x') = \delta^{\mu 0}\delta^{\nu 0}\delta(t-t')\frac{1}{4\pi}\left(\frac{9}{5} - \frac{r^2}{2} - \frac{r'^2}{2}\right) \tag{139}$$

for the gluon propagator to find the contribution of the zero-energy scalar mode. The zero-energy scalar mode contribution to each one-gluon-exchange diagram is therefore

$$\Delta\mu_{\rm d}^{(2)} = \sum_{p\neq n_4} \frac{P_{n_3 p} M_{p n_4} \delta_{n_1 n_2}}{2(\varepsilon_4 - \varepsilon_p)}. \tag{140}$$

For the vertex correction diagram one arrives at

$$\Delta\mu_{\rm a}^{(2)} = -\sum_{\substack{\epsilon_p<0\\ p}} \frac{P_{n_1 p} M_{p n_2}}{\varepsilon_4 - \varepsilon_p}, \tag{141}$$

and for each self-energy diagram one finds

$$\Delta\mu_{\rm b}^{(2)} = -\sum_{\substack{\epsilon_p>0\\ p\neq n_4}} \frac{P_{n_1 p} M_{p n_2}}{2(\varepsilon_4 - \varepsilon_p)}. \tag{142}$$

These results are independent of the arbitrary constant c. The sum over all $O(\alpha_s)$ diagrams of the zero-energy mode is zero; thus this mode has no effect. It is, however, important to include this mode if one wishes to compare the intermediate results with work performed by other groups.

D Sum rules

D.1 Vertex correction sum rule

Although there is no way of checking the final results of the cavity QCD calculations carried out here, there are ways of carrying out independent checks on intermediate numerical results. In this appendix, a few sum rules are presented which provide a powerful means of checking the numerical sum over the complete set of intermediate cavity modes of the vertex integrals. These sum rules also demonstrate that the method of truncating the infinite sum over cavity modes is valid.

Consider, for example, the contribution from the vertex correction to the magnetic moment

$$\mu_{\rm a}^{(2)} = g^2 \int_0^\infty dz \sum_{pqm\Sigma} g^{\Sigma\Sigma}\, \tilde{Q}^{m\Sigma}_{n'p}\, M_{pq}\, Q^{m\Sigma}_{qn}\, I^{m\Sigma}_{pq}(z). \tag{143}$$

If one discards the z-dependent terms, the sum over two of the three intermediate particles may be carried out using the appropriate completeness relation. The resulting expression can be used to check that the numerical sum over those vertex integrals is functioning correctly. Choosing to sum over the quarks p and q, one has

$$V^{m\Sigma}_{nn'} \equiv 4\pi g^{\Sigma\Sigma} \sum_{pqM} \tilde{Q}^{m\Sigma}_{np}\, M_{pq}\, Q^{m\Sigma}_{qn'}, \tag{144}$$

where the sum over M runs over the gluon spin projections. Using the completeness relation for the quark cavity modes, eq. (71), the sum over p and q may be carried out immediately to give

$$V^{m\Sigma}_{nn'} = -4\pi g^{\Sigma\Sigma} \sum_M \int d^3r\, \bar{u}_n(\vec{r})\gamma_\mu\gamma_0(\vec{r}\times\vec{\gamma})_z\gamma_0\gamma_\rho u_{n'}(\vec{r})\, a^{\mu *}_{m\Sigma}(\vec{r}) a^{\rho}_{m\Sigma}(\vec{r}). \tag{145}$$

After some Dirac algebra, this yields

$$V^{m\Sigma}_{nn'} = -4\pi g^{\Sigma\Sigma} \sum_M \int d^3r\, u_n(r)\left\{ \left|a_{m\Sigma}(\vec{r})\right|^2 \left(\vec{r}\times\vec{\gamma}\right)_z + 2\left(\vec{r}\times\vec{a}_{m\Sigma}(\vec{r})\right)_z \not{a}^*_{m\Sigma}(\vec{r}) \right\} u_{n'}(\vec{r}). \tag{146}$$

If the gluon fields are now expanded in terms of vector spherical harmonics and Bessel functions, the sum over the gluon spins in eq. (146) can be evaluated. After some tedious algebra we arrive at

$$V^{m\Sigma}_{nn'} = -A_{\kappa\kappa'} \int_0^R dr\, r^3 \Big[f_n(r) g_{n'}(r) + g_n(r) f_{n'}(r) \Big] \Phi_{m\Sigma}(r), \tag{147}$$

where $A_{\kappa\kappa'}$ is the angular integral defined by eq. (116), $g_n(r)$ and $f_n(r)$ are the upper and lower components of the quark wave function, and $\Phi_{m\Sigma}(r)$ is given by

$$\Phi_{m\mathcal{S}}(r) = (2J+1)N_{m\mathcal{S}}^2 j_J^2(\Omega r) \tag{148}$$

$$\Phi_{m\mathcal{L}}(r) = \frac{N_{m\mathcal{L}}^2}{2J+1}\Big[(J+1)\,j_{J+1}(\Omega r) - J j_{J-1}(\Omega r)\Big]^2 \tag{149}$$

$$\Phi_{m\mathcal{M}}(r) = 0 \tag{150}$$

$$\Phi_{m\mathcal{E}}(r) = J(J+1)(2J+1)N_{m\mathcal{E}}^2\left(\frac{j_J(\Omega r)}{\Omega r}\right)^2. \tag{151}$$

Equation (147) can readily be evaluated numerically after choosing the quantum numbers $m\Sigma$ of the intermediate gluon, and the n and n' of the initial and final quarks.

In a similar fashion, sum rules can be derived for the contribution of the vertex correction to other operators. For the axial vector coupling constant, we obtain

$$4\pi g^{\Sigma\Sigma}\sum_{pqM}\tilde{Q}_{np}^{m\Sigma}\,G_{pq}\,Q_{qn'}^{m\Sigma} = A_{\kappa\kappa'}\int_0^R dr\,r^2\Big[\Big\{f_n(r)f_{n'}(r)+g_n(r)g_{n'}(r)\Big\}\Theta_{m\Sigma}(r)$$
$$+\,2\kappa\Big\{f_n(r)f_{n'}(r)-g_n(r)g_{n'}(r)\Big\}\Phi_{m\Sigma}(r)\Big], \tag{152}$$

where $\Phi_{m\Sigma}(r)$ is defined above, and $\Theta_{m\Sigma}(r)$ is given by

$$\Theta_{m\mathcal{S}}(r) = (2J+1)N_{m\mathcal{S}}^2 j_J^2(\Omega r)$$

$$\Theta_{m\mathcal{L}}(r) = \frac{N_{m\mathcal{L}}^2}{2J+1}\Big[J j_{J-1}^2(\Omega r)+4J(J+1)j_{J-1}(\Omega r)j_{J+1}(\Omega r)-(J+1)\,j_{J+1}^2(\Omega r)\Big]$$

$$\Theta_{m\mathcal{M}}(r) = (2J+1)N_{m\mathcal{M}}^2 j_J^2(\Omega r)$$

$$\Theta_{m\mathcal{E}}(r) = \frac{N_{m\mathcal{E}}^2}{2J+1}\Big[(J+1)j_{J-1}^2(\Omega r)-4J(J+1)j_{J-1}(\Omega r)j_{J+1}(\Omega r)-J j_{J+1}^2(\Omega r)\Big].$$

The sum of vertex integrals for the axial vector charge radius obeys a similar sum rule to that above, with the only difference being the that r^2 is replaced with r^4. Finally, a sum rule for the electromagnetic charge radius is

$$4\pi g^{\Sigma\Sigma}\sum_{pqM}\tilde{Q}_{np}^{m\Sigma}\,P_{pq}\,Q_{qn'}^{m\Sigma} = -\int_0^R dr\,r^4\Big[f_n(r)f_{n'}(r)+g_n(r)g_{n'}(r)\Big]\Upsilon_{m\Sigma}(r), \tag{153}$$

where the function $\Upsilon_{m\Sigma}(r)$ is given by

$$\Upsilon_{m\mathcal{S}}(r) = (2J+1)N_{m\mathcal{S}}^2 j_J^2(\Omega r) \tag{154}$$

$$\Upsilon_{m\mathcal{L}}(r) = -N_{m\mathcal{L}}^2\Big[(J+1)j_{J+1}^2(\Omega r)+J j_{J-1}^2(\Omega r)\Big] \tag{155}$$

$$\Upsilon_{m\mathcal{M}}(r) = -(2J+1)N_{m\mathcal{M}}^2 j_J^2(\Omega r) \tag{156}$$

$$\Upsilon_{m\mathcal{E}}(r) = -N_{m\mathcal{E}}^2\Big[J j_{J+1}^2(\Omega r)+(J+1)j_{J-1}^2(\Omega r)\Big]. \tag{157}$$

D.2 Sum rule for the self-energy inserts

The vertex diagrams with a self-energy insert on one of the external legs yield similar sum rules to the vertex correction diagrams. In fact, the sum rule for the electromagnetic charge radius is the same for both diagrams. For the magnetic moment, one obtains

$$4\pi g^{\Sigma\Sigma}\sum_{pqM}\tilde{Q}_{np}^{m\Sigma}\,Q_{pq}^{m\Sigma}\,M_{qn'} = -A_{\kappa\kappa'}\int_0^R dr\,r^3\Big[f_n(r)g_{n'}(r)+g_n(r)f_{n'}(r)\Big]\Upsilon_{m\Sigma}(r), \tag{158}$$

while the result for the axial vector coupling constant is

$$4\pi g^{\Sigma\Sigma}\sum_{pqM}\tilde{Q}_{np}^{m\Sigma}\,Q_{pq}^{m\Sigma}\,G_{qn'} = \tag{159}$$
$$= -A_{\kappa\kappa'}\int_0^R dr\,r^2\Big[(\kappa+\kappa'-1)g_n(r)g_{n'}(r)-(\kappa+\kappa'+1)f_n(r)f_{n'}(r)\Big]\Upsilon_{m\Sigma}(r),$$

where the $\Upsilon_{m\Sigma}(r)$ were defined in eqs. (154) to (157).

D.3 One-gluon exchange sum rules

In a similar way, sum rules for the diagrams involving gluon exchange between quarks may be derived. Unfortunately, these sum rules tend to be rather lengthy, since they depend on the the quantum numbers of two initial and two final state quarks.

Consider the expression for the one-gluon exchange correction to the electromagnetic charge radius. The part which contains the sum over the vertex integrals is defined

as

$$W_{n_1n_2n_3n_4} \equiv 4\pi g^{\Sigma\Sigma} \sum_{pm\Sigma} \tilde{Q}^{m\Sigma}_{n_1n_2}\, Q^{m\Sigma}_{n_3p}\, P_{pn_4}. \tag{160}$$

Both of the intermediate particles may be summed over using the quark and gluon completeness relations, eqs. (71) and (89), yielding

$$W_{n_1n_2n_3n_4} = -4\pi \int d^3r\, |\vec{r}|^2\, \bar{u}_{n_1}(\vec{r})\gamma_\mu u_{n_2}(\vec{r})\, \bar{u}_{n_3}(\vec{r})\gamma^\mu u_{n_4}(\vec{r}). \tag{161}$$

After multiplying out the spinors, we arrive at

$$W_{n_1n_2n_3n_4} = \int dr\, r^4 \Big[-\Big(g_{n_1}f_{n_2} + g_{n_2}f_{n_1}\Big)\Big(g_{n_3}f_{n_4} + g_{n_4}f_{n_3}\Big) A_{\kappa_1-\kappa_2\kappa_3-\kappa_4} \tag{162}$$

$$+ \Big\{ 2g_{n_1}f_{n_2}f_{n_3}g_{n_4} + 2f_{n_1}g_{n_2}g_{n_3}f_{n_4} - (g_{n_1}g_{n_2} + f_{n_1}f_{n_2})(g_{n_3}g_{n_4} + f_{n_3}f_{n_4}) \Big\} B_{\kappa_1\kappa_2\kappa_3\kappa_4} \Big],$$

where $A_{\kappa_1\kappa_2\kappa_3\kappa_4}$ and $B_{\kappa_1\kappa_2\kappa_3\kappa_4}$ are the angular integrals, i.e.

$$\begin{aligned} A_{\kappa_1\kappa_2\kappa_3\kappa_4} &\equiv 4\pi \int d\hat{r}\, \Big(\chi^{\mu_1\dagger}_{\kappa_1}(\hat{r})\, \vec{\sigma}\, \chi^{\mu_2}_{\kappa_2}(\hat{r})\Big) \cdot \Big(\chi^{\mu_3\dagger}_{\kappa_3}(\hat{r})\, \vec{\sigma}\, \chi^{\mu_4}_{\kappa_4}(\hat{r})\Big) \\ &= 6\hat{j}_1\hat{j}_2\hat{j}_3\hat{j}_4\hat{\ell}_1\hat{\ell}_2\hat{\ell}_3\hat{\ell}_4 \sum_{JL} (-1)^{J-L+j_1+j_3-\ell_2-\ell_4+\mu_3-\mu_2}(2J+1)(2L+1) \\ &\begin{pmatrix} j_1 & j_2 & J \\ -\mu_1 & \mu_2 & \mu_1-\mu_2 \end{pmatrix} \begin{pmatrix} j_3 & j_4 & J \\ -\mu_3 & \mu_4 & \mu_2-\mu_1 \end{pmatrix} \begin{pmatrix} \ell_1 & \ell_2 & L \\ 0 & 0 & 0 \end{pmatrix} \begin{pmatrix} \ell_3 & \ell_4 & L \\ 0 & 0 & 0 \end{pmatrix} \\ &\begin{Bmatrix} \ell_1 & j_1 & \frac{1}{2} \\ \ell_2 & j_2 & \frac{1}{2} \\ L & J & 1 \end{Bmatrix} \begin{Bmatrix} \ell_3 & j_3 & \frac{1}{2} \\ \ell_4 & j_4 & \frac{1}{2} \\ L & J & 1 \end{Bmatrix}, \end{aligned} \tag{163}$$

where the shorthand $\hat{j} = \sqrt{2j+1}$ has been used, and

$$\begin{aligned} B_{\kappa_1\kappa_2\kappa_3\kappa_4} &\equiv 4\pi \int d\hat{r}\, \chi^{\mu_1\dagger}_{\kappa_1}(\hat{r})\, \chi^{\mu_2}_{\kappa_2}(\hat{r})\, \chi^{\mu_3\dagger}_{\kappa_3}(\hat{r})\, \chi^{\mu_4}_{\kappa_4}(\hat{r}) \\ &= (-1)^{\ell_1-\ell_2+\ell_3-\ell_4}\, \hat{j}_1\hat{j}_2\hat{j}_3\hat{j}_4 \sum_J (2J+1) \frac{1+(-1)^{\ell_1+\ell_2+J}}{2}\, \frac{1+(-1)^{\ell_3+\ell_4+J}}{2} \\ &\begin{pmatrix} j_1 & j_2 & J \\ -\mu_1 & \mu_2 & \mu_1-\mu_2 \end{pmatrix} \begin{pmatrix} j_3 & j_4 & J \\ -\mu_3 & \mu_4 & \mu_2-\mu_1 \end{pmatrix} \begin{pmatrix} j_1 & j_2 & J \\ \frac{1}{2} & -\frac{1}{2} & 0 \end{pmatrix} \begin{pmatrix} j_3 & j_4 & J \\ \frac{1}{2} & -\frac{1}{2} & 0 \end{pmatrix}. \end{aligned} \tag{164}$$

The sum rule for the magnetic moment can be derived in the same way. It is given by

$$4\pi g^{\Sigma\Sigma} \sum_{pm\Sigma} \tilde{Q}^{m\Sigma}_{n_1n_2}\, Q^{m\Sigma}_{n_3p}\, M_{pn_4} = \tag{165}$$

$$\int dr\, r^3 \Big[\Big(g_{n_1}f_{n_2} + g_{n_2}f_{n_1}\Big)\Big(g_{n_3}g_{n_4} + f_{n_4}f_{n_3}\Big)\Big(\tfrac{1}{2}C_{\kappa_3\kappa_4\kappa_1\kappa_2} - \tfrac{1}{2}C_{\kappa_1-\kappa_2\kappa_3-\kappa_4} + D_{\kappa_3\kappa_4\kappa_1-\kappa_2}\Big)$$

$$+ \Big\{ 2g_{n_1}f_{n_2}f_{n_3}f_{n_4} + 2f_{n_1}g_{n_2}g_{n_3}g_{n_4} - (g_{n_1}g_{n_2} + f_{n_1}f_{n_2})(g_{n_3}f_{n_4} + g_{n_4}f_{n_3}) \Big\} D_{\kappa_1\kappa_2\kappa_3-\kappa_4} \Big].$$

In this case, the angular integrals are

$$\begin{aligned} C_{\kappa_1\kappa_2\kappa_3\kappa_4} &\equiv 4\pi \int d\hat{r}\, \chi^{\mu_1\dagger}_{\kappa_1}(\hat{r})\, \sigma_z\, \chi^{\mu_2}_{\kappa_2}(\hat{r})\, \chi^{\mu_3\dagger}_{\kappa_3}(\hat{r}) \chi^{\mu_4}_{\kappa_4}(\hat{r}) = \hat{j}_1\hat{j}_2\hat{j}_3\hat{j}_4\hat{\ell}_1\hat{\ell}_2 \sum_{mL} (-1)^{L+\mu_1+\mu_3}\hat{L}^2 \\ &\begin{pmatrix} \ell_1 & \frac{1}{2} & j_1 \\ \mu_1-m & m & -\mu_1 \end{pmatrix} \begin{pmatrix} \ell_2 & \frac{1}{2} & j_2 \\ \mu_2-m & m & -\mu_2 \end{pmatrix} \begin{pmatrix} \ell_1 & L & \ell_2 \\ m-\mu_1 & \mu_1-\mu_2 & \mu_2-m \end{pmatrix} \\ &\begin{pmatrix} j_3 & L & j_4 \\ -\mu_3 & \mu_2-\mu_1 & \mu_4 \end{pmatrix} \begin{pmatrix} j_3 & L & j_4 \\ \frac{1}{2} & 0 & -\frac{1}{2} \end{pmatrix} \begin{pmatrix} \ell_1 & \ell_2 & L \\ 0 & 0 & 0 \end{pmatrix} \frac{1+(-1)^{\ell_3+L+\ell_4}}{2}. \end{aligned} \tag{166}$$

The other integral needed here is given by

$$\begin{aligned} D_{\kappa_1\kappa_2\kappa_3\kappa_4} &\equiv 4\pi i \int d\hat{r}\, \chi^{\mu_1\dagger}_{\kappa_1}(\hat{r})\chi^{\mu_2}_{\kappa_2}(\hat{r})\, \chi^{\mu_3\dagger}_{\kappa_3}(\hat{r})(\hat{r}\times\vec{\sigma})_z\chi^{\mu_4}_{\kappa_4}(\hat{r}) = \frac{1}{\sqrt{2}}(-1)^{\mu_2+\mu_4}\hat{j}_1\hat{j}_2\hat{j}_3\hat{j}_4 \\ &\sum_{mm'LL'} (-1)^{L+L'-m-m'}\, \hat{L}^2\hat{L}'^2 \begin{pmatrix} \ell_1 & \frac{1}{2} & j_1 \\ \mu_1-m & m & -\mu_1 \end{pmatrix} \begin{pmatrix} \ell_2 & \frac{1}{2} & j_2 \\ \mu_2-m & m & -\mu_2 \end{pmatrix} \\ &\begin{pmatrix} \ell_3 & \frac{1}{2} & j_3 \\ \mu_3+m' & -m' & -\mu_3 \end{pmatrix} \begin{pmatrix} \ell_4 & \frac{1}{2} & j_4 \\ \mu_4-m' & m' & -\mu_4 \end{pmatrix} \begin{pmatrix} \ell_1 & \ell_2 & L \\ 0 & 0 & 0 \end{pmatrix} \\ &\begin{pmatrix} \ell_1 & L & \ell_2 \\ m-\mu_1 & \mu_4-\mu_3 & \mu_2-m \end{pmatrix} \begin{pmatrix} \ell_3 & L' & \ell_4 \\ -\mu_3-m' & \mu_3-\mu_4+2m' & \mu_4-m' \end{pmatrix} \\ &\begin{pmatrix} \ell_3 & \ell_4 & L' \\ 0 & 0 & 0 \end{pmatrix} \begin{pmatrix} L' & 1 & L \\ 0 & 0 & 0 \end{pmatrix} \begin{pmatrix} L' & 1 & L \\ \mu_4-\mu_3-2m' & 2m' & \mu_3-\mu_4 \end{pmatrix} \hat{\ell}_1\hat{\ell}_2\hat{\ell}_3\hat{\ell}_4. \end{aligned} \tag{167}$$

Finally, the sum rule for the axial vector coupling constant is

$$\begin{aligned} 4\pi g^{\Sigma\Sigma} \sum_{pm\Sigma} \tilde{Q}^{m\Sigma}_{n_1n_2}\, Q^{m\Sigma}_{n_3p}\, G_{pn_4} = \int dr\, r^2 \Big[& g_{n_1}f_{n_2}\Big(f_{n_3}g_{n_4}E_{\kappa_1-\kappa_2-\kappa_3\kappa_4} - g_{n_3}f_{n_4}E_{\kappa_1-\kappa_2\kappa_3-\kappa_4}\Big) \\ & - \Big(g_{n_1}g_{n_2} + f_{n_1}f_{n_1}\Big)\Big(g_{n_3}g_{n_4}C_{\kappa_3\kappa_4\kappa_1\kappa_2} + f_{n_3}f_{n_4}C_{-\kappa_3-\kappa_4\kappa_1\kappa_2}\Big) \\ & + f_{n_1}g_{n_2}\Big(g_{n_3}f_{n_4}E_{-\kappa_1\kappa_2\kappa_3-\kappa_4} - f_{n_3}g_{n_4}E_{-\kappa_1\kappa_2-\kappa_3\kappa_4}\Big)\Big]. \end{aligned} \tag{168}$$

The angular integral $E_{\kappa_1\kappa_2\kappa_3\kappa_4}$ is defined by

$$E_{\kappa_1\kappa_2\kappa_3\kappa_4} \equiv 4\pi \int d\hat{r}\, \chi^{\mu_1\dagger}_{\kappa_1}(\hat{r})\, \vec{\sigma}\, \chi^{\mu_2}_{\kappa_2}(\hat{r}) \cdot \chi^{\mu_3\dagger}_{\kappa_3}(\hat{r})\, \vec{\sigma}\sigma_z\, \chi^{\mu_4}_{\kappa_4}(\hat{r}) = 2\hat{j}_1\,\hat{j}_2\,\hat{j}_3\,\hat{j}_4\,\hat{\ell}_1\,\hat{\ell}_2\,\hat{\ell}_3\,\hat{\ell}_4 \times$$

$$\sum_{mL} (-1)^{\mu_2-\mu_3-m+1/2}\,(2L+1) \begin{pmatrix} \ell_1 & \frac{1}{2} & j_1 \\ \mu_1 - m & m & -\mu_1 \end{pmatrix} \begin{pmatrix} \ell_2 & \frac{1}{2} & j_2 \\ \mu_2 + m & -m & -\mu_2 \end{pmatrix}$$

$$\begin{pmatrix} \ell_3 & \frac{1}{2} & j_3 \\ \mu_3 + m & -m & -\mu_3 \end{pmatrix} \begin{pmatrix} \ell_4 & \frac{1}{2} & j_4 \\ \mu_4 - m & m & -\mu_4 \end{pmatrix} \begin{pmatrix} \ell_1 & \ell_2 & L \\ 0 & 0 & 0 \end{pmatrix} \begin{pmatrix} \ell_3 & \ell_4 & L \\ 0 & 0 & 0 \end{pmatrix}$$

$$\begin{pmatrix} \ell_1 & \ell_2 & L \\ m - \mu_1 & m + \mu_2 & \mu_1 - \mu_2 - 2m \end{pmatrix} \begin{pmatrix} \ell_3 & \ell_4 & L \\ m + \mu_3 & m - \mu_4 & \mu_4 - \mu_3 - 2m \end{pmatrix}$$

$$+\, C_{\kappa_1\kappa_2\kappa_3\kappa_4}. \tag{169}$$

Note that the completeness relation for the gluon modes, eq. (89), includes the zero-energy scalar mode, which has the quantum numbers $m\Sigma = m_0\mathcal{S}$, where $m_0 = \{N = 0, J = 0, M = 0\}$. The contribution of this term to the left-hand side of the one-gluon exchange sum rules above may be calculated separately, and added to the numerical sum. One finds that

$$4\pi g^{\mathcal{SS}} \sum_p \tilde{Q}^{m_0\mathcal{S}}_{n_1n_2}\, Q^{m_0\mathcal{S}}_{n_3p}\, M_{pn_4} = -3\delta_{n_1n_2} M_{n_3n_4}. \tag{170}$$

E Colour and flavour matrix elements

E.1 One-body terms

The matrix elements of the external operator and quark creation/annihilation operators between proton and neutron states will be derived here. There are two distinct types of these matrix elements, corresponding to the one- and two-body interactions.

The colour and flavour matrix elements for the one-body interaction to be evaluated are given by

$$\sum_{cc'dff'n} \left\langle \hat{p} \middle| \hat{a}^\dagger_{c'f'n} \left(\frac{\lambda^a}{2}\right)_{c'd} \left(\frac{\lambda^a}{2}\right)_{dc} Q\, \hat{a}_{cfn} \middle| \hat{p} \right\rangle, \tag{171}$$

where $|\hat{p}\rangle$ is the wave function for spin-up protons, given in second quantized form by

$$\left|\hat{p}\right\rangle = \frac{\varepsilon^{abc}}{\sqrt{18}} \left(a^\dagger_{a,u,1s\uparrow}\, a^\dagger_{b,d,1s\downarrow} - a^\dagger_{a,u,1s\downarrow}\, a^\dagger_{b,d,1s\uparrow} \right) a^\dagger_{c,u,1s\uparrow} \left|\hat{0}\right\rangle. \tag{172}$$

The operator $\hat{a}^\dagger_{a,u,1s\uparrow}$ creates a spin-up quark with colour a and flavour u in the $1s$ state, and ε^{abc} is the completely anti-symmetric tensor of rank 3. The charge matrix Q for u and d quarks may be written in terms of the unit and isospin matrices as

$$Q = \tfrac{1}{6}\left(I + 3\tau_3\right). \tag{173}$$

The action of the diagonal matrices I and τ_3 can be represented by δ-functions which restrict the flavour f of the quark to either u or d.

$$\begin{aligned} I &= \delta_{f,u} + \delta_{f,d} \\ \tau_3 &= \delta_{f,u} - \delta_{f,d}. \end{aligned} \tag{174}$$

The operator Q does not change the colour or flavour of the quarks on either side of its vertex, since it interacts only through the colourless electromagnetic field. In other words, $c' = c$ and $f' = f$ on either side of the operator insert. Hence, after noting the standard relation

$$\sum_d \left(\frac{\lambda^a}{2}\right)_{c'd} \left(\frac{\lambda^a}{2}\right)_{dc} = \frac{4}{3}\delta_{c'c}, \tag{175}$$

the expression for the colour and flavour matrix elements becomes

$$\sum_{cc'dff'n} \left\langle \hat{p} \left| \hat{a}^{\dagger}_{c'f'n} \left(\frac{\lambda^a}{2}\right)_{c'd} \left(\frac{\lambda^a}{2}\right)_{dc} Q\, \hat{a}_{cfn} \right| \hat{p} \right\rangle = \frac{4}{3} \sum_{cfn} \left\langle \hat{p} \left| a^{\dagger}_{cfn}\, Q\, a_{cfn} \right| \hat{p} \right\rangle. \quad (176)$$

Using the anti-commutation relations for the creation and annihilation operators

$$\left\{ a_{cfn}\,,\, a^{\dagger}_{c'f'n'} \right\} = \delta_{cc'}\, \delta_{ff'}\, \delta_{nn'}, \quad (177)$$

the sum over colours and flavours may be carried out by anti-commuting the annihilation operators to the right and the creation operators to the left, through the wave function, until the vacuum state is reached. The operators vanish at this point since $a_{cn}|\hat{0}\rangle = 0$ and $\langle\hat{0}|a^{\dagger}_{cn} = 0$. These sums and ordering operations can be carried out on a computer using REDUCE 3.3, and can take a surprisingly long time on, although the matrix elements of I and τ_3 turn out to be quite simple. The results are

$$\sum_{cfn} \left\langle \hat{p} \left| a^{\dagger}_{cfn}\, I\, a_{cfn} \right| \hat{p} \right\rangle = (2\delta_{\mu,\uparrow} + \delta_{\mu,\downarrow})\delta_{n,1s} \quad (178)$$

$$\sum_{cfn} \left\langle \hat{p} \left| a^{\dagger}_{cfn}\, \tau_3\, a_{cfn} \right| \hat{p} \right\rangle = \frac{1}{3}(4\delta_{\mu,\uparrow} - \delta_{\mu,\downarrow})\delta_{n,1s}. \quad (179)$$

The matrix elements of Q can immediately be found by using these expressions and the definition of Q, eq. (173). The final expression is

$$\sum_{cfn} \left\langle \hat{p} \left| \hat{a}^{\dagger}_{c'fn} \left(\frac{\lambda^a}{2}\right)_{c'd} \left(\frac{\lambda^a}{2}\right)_{dc} Q\, \hat{a}_{cfn} \right| \hat{p} \right\rangle = \frac{4}{3}\, \delta_{\mu,\uparrow}\, \delta_{n,1s}. \quad (180)$$

The corresponding colour and flavour matrix elements taken between neutron states are

$$\sum_{cfn} \left\langle \hat{n} \left| \hat{a}^{\dagger}_{c'fn} \left(\frac{\lambda^a}{2}\right)_{c'd} \left(\frac{\lambda^a}{2}\right)_{dc} Q\, \hat{a}_{cfn} \right| \hat{n} \right\rangle = -\frac{4}{9}\left(\delta_{\mu,\uparrow} - \delta_{\mu,\downarrow}\right)\delta_{r,1s}. \quad (181)$$

E.2 Two-body terms

The two-body matrix elements arising from the one-gluon exchange diagrams are given by

$$\sum_{\substack{\text{colours}\\ \text{flavours}}} \left\langle \hat{p} \left| \hat{a}^{\dagger}_{c'f'n_1} \hat{a}^{\dagger}_{d'g'n_3} \left(\frac{\lambda^a}{2}\right)_{c'c} \left(\frac{\lambda^a}{2}\right)_{d'd} Q\, \hat{a}_{cfn_2} \hat{a}_{dgn_4} \right| \hat{p} \right\rangle. \quad (182)$$

The gluon which is exchanged between the two quark lines $n_2 n_1$ and $n_4 n_3$ carries no flavour, and neither does the external operator attached to the line $n_4 n_3$, so the flavour cannot change along either of these lines. Hence, $f' = f$ and $g' = g$. Using the colour factor from the λ^a matrices

$$\left(\frac{\lambda^a}{2}\right)_{c'c} \left(\frac{\lambda^a}{2}\right)_{d'd} = \frac{1}{2}\left(\delta_{c'd}\, \delta_{cd'} - \frac{1}{3}\, \delta_{c'c}\, \delta_{d'd}\right), \quad (183)$$

the sum over all allowed colours, flavours and radial states of the matrix element for I is found to be

$$\begin{aligned} &\sum_{\substack{\text{colours}\\ \text{flavours}}} \left\langle \hat{p} \left| \hat{a}^{\dagger}_{c'fn_1} \hat{a}^{\dagger}_{d'gn_3} \left(\frac{\lambda^a}{2}\right)_{c'c} \left(\frac{\lambda^a}{2}\right)_{d'd} I\, \hat{a}_{cfn_2} \hat{a}_{dgn_4} \right| \hat{p} \right\rangle \\ &= \frac{2}{3}\Big[\left(\delta_{\mu_1\mu_3,\uparrow} + 2\delta_{\mu_1,\uparrow}\, \delta_{\mu_3,\downarrow} + 2\delta_{\mu_1,\downarrow}\, \delta_{\mu_3,\uparrow}\right)\delta_{\mu_1,\mu_2}\, \delta_{\mu_3,\mu_4} \\ &\quad + \left(\delta_{\mu_1\mu_3,\uparrow} - \delta_{\mu_1,\uparrow}\, \delta_{\mu_3,\downarrow} - \delta_{\mu_1,\downarrow}\, \delta_{\mu_3,\uparrow}\right)\delta_{\mu_2,\mu_3}\, \delta_{\mu_1,\mu_4}\Big]\delta_{n_1 n_2 n_3 n_4, 1s}, \end{aligned} \quad (184)$$

where a shorthand notation for repeated δ-functions having one argument in common has been introduced

$$\delta_{ab\cdots c,z} \equiv \delta_{a,z}\, \delta_{b,z} \cdots \delta_{c,z}. \quad (185)$$

Similarly, the matrix element containing the operator τ_3 is found to be

$$\begin{aligned} &\sum_{\substack{\text{colours}\\ \text{flavours}}} \left\langle \hat{p} \left| \hat{a}^{\dagger}_{c'fn_1} \hat{a}^{\dagger}_{d'gn_3} \left(\frac{\lambda^a}{2}\right)_{c'c} \left(\frac{\lambda^a}{2}\right)_{d'd} \tau_3\, \hat{a}_{cfn_2} \hat{a}_{dgn_4} \right| \hat{p} \right\rangle \\ &= \frac{2}{9}\Big[2\left(\delta_{\mu_1\mu_3,\uparrow} + 2\delta_{\mu_1,\downarrow}\, \delta_{\mu_3,\uparrow} - \delta_{\mu_1,\uparrow}\, \delta_{\mu_3,\downarrow}\right)\delta_{\mu_1,\mu_2}\, \delta_{\mu_3,\mu_4} \\ &\quad + \left(2\delta_{\mu_1\mu_3,\uparrow} + \delta_{\mu_1,\downarrow}\, \delta_{\mu_3,\uparrow} + \delta_{\mu_1,\uparrow}\, \delta_{\mu_3,\downarrow}\right)\delta_{\mu_2,\mu_3}\, \delta_{\mu_1,\mu_4}\Big]\delta_{n_1 n_2 n_3 n_4, 1s}. \end{aligned} \quad (186)$$

A considerable simplification results when these two matrix elements, in conjunction with the definition of Q in eq. (173), are added together. The final result for the matrix element of Q is

$$\begin{aligned} &\sum_{\substack{\text{colours}\\ \text{flavours}}} \left\langle \hat{p} \left| \hat{a}^{\dagger}_{c'fn_1} \hat{a}^{\dagger}_{d'gn_3} \left(\frac{\lambda^a}{2}\right)_{c'c} \left(\frac{\lambda^a}{2}\right)_{d'd} Q\, \hat{a}_{cfn_2} \hat{a}_{dgn_4} \right| \hat{p} \right\rangle \\ &= \frac{2}{3}\left(\delta_{\mu_1\mu_2,\uparrow} + \delta_{\mu_1\mu_2,\downarrow}\right)\delta_{\mu_3\mu_4,\uparrow}\, \delta_{n_1 n_2 n_3 n_4, 1s} \end{aligned} \quad (187)$$

In a similar manner, the matrix elements of the colour, flavour and charge operators of a two-body state taken between neutron wave functions yield

$$\sum_{\substack{\text{colours}\\ \text{flavours}}} \left\langle \hat{n} \left| \hat{a}^{\dagger}_{c'fn_1} \hat{a}^{\dagger}_{d'gn_3} \left(\frac{\lambda^a}{2}\right)_{c'c} \left(\frac{\lambda^a}{2}\right)_{d'd} Q\, \hat{a}_{cfn_2} \hat{a}_{dgn_4} \right| \hat{n} \right\rangle$$

$$= \frac{1}{9}\Big[\Big(4\delta_{\mu_1,\uparrow}\,\delta_{\mu_3,\downarrow} - 2\delta_{\mu_1,\downarrow}\,\delta_{\mu_3,\uparrow} - \delta_{\mu_1\mu_3,\uparrow}\Big)\delta_{\mu_1,\mu_2}\,\delta_{\mu_3,\mu_4} \tag{188}$$

$$- \Big(2\delta_{\mu_1,\uparrow}\,\delta_{\mu_3,\downarrow} + 2\delta_{\mu_1,\downarrow}\,\delta_{\mu_3,\uparrow} + \delta_{\mu_1\mu_3,\uparrow}\Big)\delta_{\mu_2,\mu_3}\,\delta_{\mu_1,\mu_4}\Big]\delta_{n_1n_2n_3n_4,1s}.$$

References

[1] A. CHODOS, R. L. JAFFE, K. JOHNSON, C.B. THORN and V. F. WEISSKOPF, *Phys. Rev.* **D9** (1974) 3471; A. CHODOS, R. L. JAFFE, K. JOHNSON and C.B. THORN *Phys. Rev.* **D10** (1974) 2599; T. DEGRAND, R. L. JAFFE, K. JOHNSON and J. KISKIS *Phys. Rev.* **D12** (1975) 2060.

[2] F.E. CLOSE and R.R. HORGAN, *Nucl. Phys.* **B164** (1980) 413.

[3] G. E. BROWN and M. RHO, *Phys. Lett.* **B82** (1979) 177; G. E. BROWN, M. RHO and V. VENTO, *Phys. Lett.* **B84** (1979) 383; A. W. THOMAS, *Adv. Nucl. Phys.* **13** (1983) 1.

[4] A. J. STODDART and R. D. VIOLLIER, *Phys. Lett.* **B208** (1988) 55

[5] J.D. BREIT, Columbia University report No. CU-TP-229 (1982) unpublished; and in: Workshop on non-perturbative quantum chromodynamics, K.A. Milton (Birkhäuser, Basel, 1983) p.45.

[6] S. A. CHIN, A. K. KERMAN and X. H. YANG, MIT preprint CTP No. 919 (1981).

[7] S. GOLDHABER, T. H. HANSSON and R. L. JAFFE, *Phys. Lett.* **B131** (1983) 445; *Nucl. Phys.* **B277** (1986) 674.

[8] A. J. STODDART and R. D. VIOLLIER, *Phys. Lett.* **B236** (1990) 387; *Nucl. Phys.* **A532** (1991) 657; *Nucl. Phys.* **A541** (1992) 623.

[9] P.R. PAGE, R.J. LINDEBAUM and R. D. VIOLLIER, *Nucl. Phys.* **A560** (1993) 1003

[10] O. V. MAXWELL and V. VENTO, *Nucl. Phys.* **A407** (1983) 366.

[11] J. A. CUTHBERT and R. D. VIOLLIER, *Z. Phys.* **C58** (1992) 132.

[12] G. U. SCHREIBER and R. D. VIOLLIER, *Phys. Lett.* **B279** (1992) 131; G. U. SCHREIBER and R. D. VIOLLIER, *Ann. Phys.* **215** (1992) 277.

[13] T. H. HANSSON and R. L. JAFFE, *Phys. Rev.* **D28** (1983) 882.

[14] T. H. HANSSON and R. L. JAFFE, *Ann. Phys.* **151** (1983) 204.

[15] A. L. FETTER and J. D. WALECKA, *Quantum Theory of Many Particle Systems* (McGraw-Hill, New York, 1971).

[16] J. SUCHER, *Phys. Rev.* **107** (1957) 1448.

[17] PARTICLE DATA GROUP, *Phys. Rev.* **D45** (1992) 1.

[18] K. TSUSHIMA, T. YAMAGUCHI, Y. KOHYAMA and K. KUBODERA, *Nucl. Phys.* **A489** (1988) 557.

[19] K. USHIO, *Phys. Lett.* **B158** (1985) 71; K. USHIO, *Z. Phys.* **C30** (1986) 115.

[20] M. I. KRIVORUCHENKO, *Sov. J. Nucl. Phys.* **40** (1984) 514; I. Yu. KOBZAREV, L. A. KONDRATYUCK, M. I. KRIVORUCHENKO, B. V. MARTEM'YANOV and M. G. SHCHEPKIN, *Sov. J. Nucl. Phys.* **43** (1986) 803.

[21] H. HØGAASEN and F. MYHRER, *Phys. Rev.* **D37** (1988) 1950.

[22] R. D. VIOLLIER, S. A. CHIN and A. K. KERMAN, *Nucl. Phys.* **A407** (1983) 269.

[23] R. F. BUSER, R. D. VIOLLIER and P. ZIMAK, *Int. J. Theor. Phys.* **27** (1988) 925.

[24] A. J. STODDART, *Renormalization of Cavity Field Theories*, PhD thesis, unpublished, University of Cape Town preprint UCT-TP 139/90 (1990).

[25] D. A. VARSHALOVICH, A. N. MOSKALEV and V. K. KHERSONSKII, *Quantum Theory of Angular Momentum* (World Scientific, Singapore, 1988).

[26] A. R. EDMONDS, *Angular Momentum in Quantum Mechanics* (Princeton University Press, New Jersey, 1957).

[27] T. D. LEE, *Phys. Rev.* **D19** (1979) 1802.

Figure Captions

Figure 1: Feynman diagrams contributing to the anomalous magnetic moment of a quark. The cross and dashed line denote the external electromagnetic source, and the gluons are indicated by the wavy lines.

Figure 2: Feynman diagrams contributing to the baryon magnetic moments. The intermediate quarks are labelled by p and q, and the gluon by m, Σ.

Figure 3: The vertex correction for the magnetic moment $\mu_a^{(2)}(y)$ (solid line) and the free-space divergence $\mu_S(y)$ (dashed line).

Figure 4: The two contributions to the diagram with a self-energy insert on an external leg. The dashed line shows the free-space divergence.

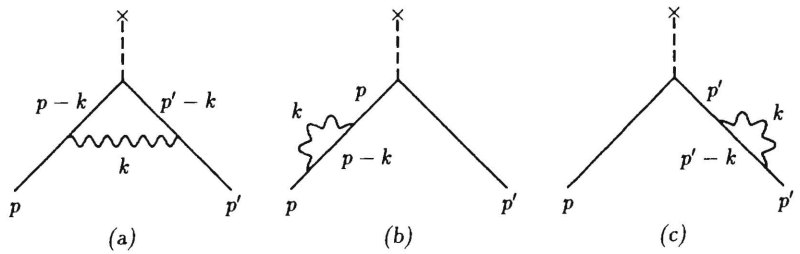

Figure 1

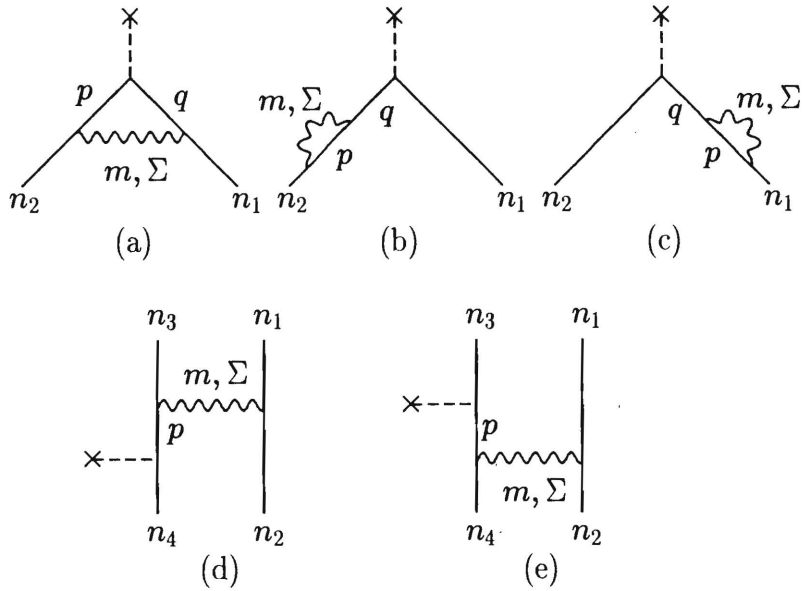

Figure 2

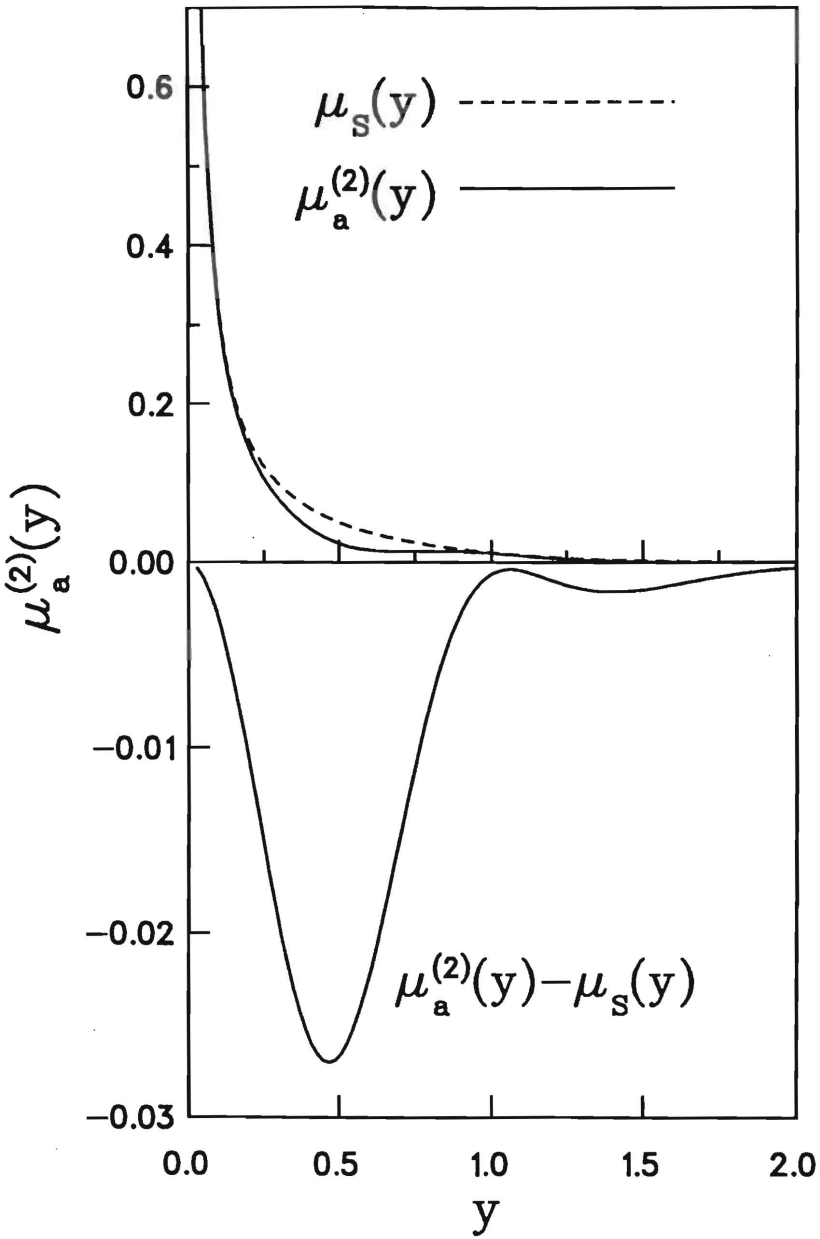

Figure 3

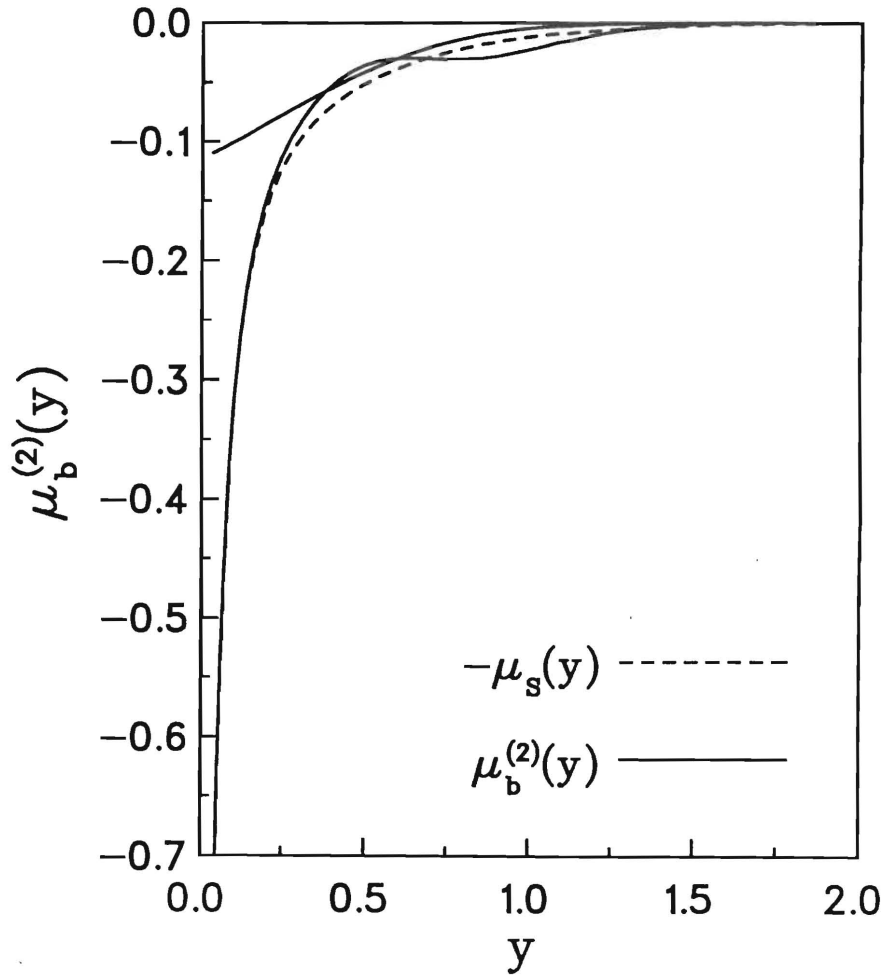

Figure 4